Draft version August 30, 2016
Preprint typeset using LaTeX style emulateapj v. 11/12/01

arXiv:1608.08012v1 [astro-ph.GA] 29 Aug 2016

FORMATION OF ANOMALOUS GLOBULAR CLUSTERS WITH METALLICITY SPREADS: A UNIFIED PICTURE

Kenji Bekki
ICRAR, M468, The University of Western Australia 35 Stirling Highway, Crawley Western Australia, 6009, Australia
AND

Takuji Tsujimoto
National Astronomical Observatory of Japan, Mitaka-shi, Tokyo 181-8588, Japan
Draft version August 30, 2016

ABSTRACT

Recent observations have revealed that at least 8 globular clusters (GCs) in the Galaxy show internal abundance spreads in [Fe/H]. We investigate the origin of these 'anomalous' GCs using numerical simulations of GCs in the dwarfs orbiting around the Galaxy and chemical evolution model of dwarfs hosting the GCs. The principal results are as follows. GCs formed in a host dwarf galaxy with a total mass of $\sim 10^{10}$M$_{\odot}$ can merge to form a single nuclear GC before the host is completely destroyed by the Galaxy, if they are massive ($> 3 \times 10^5$M$_{\odot}$) and if they are formed in the inner region ($R < 400$ pc). The GC merger remnants can capture field stars during its spiral-in to nuclear regions. If two GCs are formed from star formation events separated by ~ 300 Myr in their host dwarf, then the new GC formed from GC merging can have [Fe/H] spread of 0.2 dex and [Ba/Fe] spread of 0.3 dex. GCs formed from GC merging can show variety of internal abundance spreads depending on the details of their hosts' chemical evolution. We suggest that anomalous GCs were formed from GC merging that occurred before the destruction of GC host dwarfs yet after self-enrichment processes responsible for the observed anti-correlations between chemical abundances of light elements. We also suggest that the observed no/little dependence of [Eu/Fe] on [Fe/H] in the Galactic GC M22 is evidence of massive dwarf galaxies hosting these anomalous GCs.

Subject headings: globular cluster: general – galaxies: star clusters: general – galaxies: stellar content – stars:formation

1. INTRODUCTION

Recent photometric and spectroscopic observations of GCs have established the presence of multiple stellar populations in most of the investigated Galactic GCs (e.g., Gratton et al. 2012 for a recent review). Strong evidence for the multiple stellar populations includes, for example, the multiple main-sequence turn-offs and triple main sequence in ω Cen and NGC 2808 (e.g., Bedin et al. 2004; Piotto et al. 2005; 2007), ubiquitous anti-correlations between light elements in most Galactic GCs (e.g., Carretta et at. 2009), and internal star-to-star variations in s-process elements in some massive GCs (e.g., Yong et al. 2014; Marino et al. 2015; M15). These observations have raised a number of fundamental questions regarding the GC formation and evolution: (i) whether or not the presence of multiple stellar populations means the multiple generations of stars (e.g., Bastian et al 2013; Renzini et al. 2015), (ii) how the observed C-N and O-Na anti-correlations can be explained by theoretical models based on the self-enrichment by asymptotic giant branch stars (AGB) or fast-rotating massive stars (FRMS) in the early evolution of GCs (e.g., Decressin et al. 2007; D'Ercole et al. 2008; D08), and (iii) how multi-generation of stars can be successively formed in GCs (e.g., D08; Bekki 2011; B11).

One of the key unresolved problems related to multiple stellar populations of GCs is the origin of 'anomalous GC' with internal metallicity spreads (Δ[Fe/H]> 0.05 dex) among GC stars (See Table 10 in M15 for a nice summary of chemical properties for the 8 anomalous GCs). Each of these 8 GCs is observed to show internal spreads in chemical abundances of stars other than [Fe/H], such as C+N+O and s-process elements. For example, Marino et al. (2011) found that (i) M22 has at least two groups of stars with the [Fe/H] difference of ~ 0.15 dex among the two groups, (ii) Fe-rich group also shows a higher abundance of s-process element, and (iii) C-N and Na-O anti-correlation can be seen in each of the two groups. Yong et al. (2014) have recently revealed the presence of three distinct populations with [Fe/H] of ≈ -1.7, -1.5 and -1.0 and internal abundance spreads in s-process elements in the Galactic GC M2 and thus suggested that the formation history of M2 can be quite similar to other anomalous GCs such as ω Cen (See Lardo et al. 2013 for similar results on the abundance spread in M2). Internal abundance spreads in s-process elements, p-capture elements, and C+N+O are observed in NGC 1851 (e.g., Yong & Gundhahl (2008), Carretta et al. (2010), Villanova et al. (2010), and Youg et al. (2014).

Johnson et al. (2015) have recently investigated chemical properties of stars in NGC 6273 (M19), which is not listed as an anomalous GC in M15, and found Δ[Fe/H] of 0.5 dex among the GC stars, a significant [La/Fe] enhancement in more metal-rich stars, and a possible third metal-rich population. Lee et al. (2009) investigated the hk index in RGB sequences of 37 Galactic GCs and found that more than half of them show discrete or broad distributions of the hk index. If Δ[Ca/H] among GC stars is responsible for the observed broad hk index distribution,

then self-enrichment by supernovae needs to occur in most of GCs at their formation phases. The number of anomalous GCs appears to be currently increasing whereas the latest observations of massive GCs (e.g., NGC 2808 and 47 Tuc) does not show large [Fe/H] spreads (e.g., Carreta 2015; Milone et al. 2015; Marino et al. 2016). These imply that chemical evolution processes in forming GCs is more complicated than previous theoretical models of GC formation predicted (e.g., D'Ercole et al. 2008; B11).

In spite of these recent observational developments, theoretical studies of GC formation have not yet discussed the origin of the observed unique chemical and dynamical properties of anomalous GCs extensively. Bekki & Yong (2012, BY12) discussed the origin of the stellar halo around NGC 1851, which is one of anomalous GCs in the Galaxy, in the context of GC formation from dwarf galaxy with stellar galactic nuclei. D'Antona et al. (2016) have recently constructed a new model in which the detailed star formation history and chemical enrichment process by Type II supernovae and AGB stars are derived for explaining the observed chemical abundances of the major five stellar populations in NGC 2808. These recent theoretical studies, however, discussed either only the dynamical process of GC formation or only the chemical evolution process of forming GC. Theoretical models that can predict both various chemical abundances (e.g., $\alpha-$, $s-$, and $r-$process elements) and dynamical processes of GC formation and evolution (e.g., GC merging and tidal stripping of GC stars) are thus required for better understating the origin of the anomalous GCs.

The purpose of this paper is thus to investigate *both* dynamical evolution of GCs in host dwarf galaxies and chemical evolution of the GC hosts in order to make a more comprehensive understanding of the origin of the Galactic anomalous GCs. We adopt a new dynamical model in which both GCs and their host dwarfs are represented by N-body particles in a fully self-consistent manner so that dynamical friction of GCs against field star and dark matter, GC merging, and tidal stripping of GC stars can be investigated. Therefore, this model is significantly better than our previous model used in BY12. Furthermore, using one-zone chemical evolution models for dwarf galaxies (e.g., Tsujimoto 2011, T11; Tsujimoto & Bekki 2013; Tsujimoto & Shigeyama 2014), the present study investigates the time evolution of various chemical abundances, such as [Fe/H], [Ba/Fe], and [Eu/Fe] and their dependences on the star formation histories and the initial stellar mass function (IMF). The results can be interpreted in the context of the chemical abundances of anomalous GCs.

The plan of the paper is as follows. We describe the new dynamical evolution models of dwarf galaxies with two GCs orbiting around the Galaxy in §2. We present the numerical results on the possibility of GC merging in dwarfs and its dependence on the physical properties of GCs and dwarfs in §3. We mainly discuss whether the large spreads in [Fe/H] and s-process elements observed in the anomalous GCs can be possible in new GCs formed from GC merging using one-zone chemical evolution models in §4. We provide important implications of the present results in terms of the origin of multiple stellar populations in GCs in this section in §5. We summarize our conclusions in §6. It should be noted that we do not numerically investigate the formation of GCs from gas clouds within high-z dwarfs in the present paper: We have recently investigated how GCs can be formed from massive gas clumps formed in gas-rich dwarf galaxies using hydrodynamical simulations of dwarfs (Bekki 2016).

2. THE MODEL FOR GC MERGING

2.1. *Two-fold investigation*

We adopt the GC merging scenario for the formation of anomalous GCs, which is illustrated in Figure 1. The present study consists of (i) dynamical simulations of GC mergers in GC-host dwarf galaxies and (ii) chemical evolution study of the GC hosts. We first investigates the dynamical evolution of two GCs in massive dwarf galaxies using our own original simulation code that can be run on GPU clusters (Bekki 2013). In this first investigation, the probability of GC merging and the merging timescale of two GCs in dwarfs are discussed in detail. Although this dynamical simulations is similar to BY12, it is more sophisticated than BY12 in that (i) two GCs are represented by N-body particles in a self-consistent manner and (ii) GCs can be represented by FG+SG systems or by FG-only systems. Therefore, the present study can make more precise predictions on the dynamical fate of GCs in massive dwarfs.

We also investigate the chemical evolution of dwarfs, in particular, the evolution of [Fe/H], [s-process elements/Fe], and [r-process elements/Fe] in dwarfs, using one-zone chemical evolution models developed by T11. The present study considers that chemical abundances of anomalous GCs can reflect the chemical evolution of their host dwarfs and thereby investigates the possible spreads in the above chemical abundances within GCs. We do not discuss self-enrichment processes in the formation of SG stars from ejecta from FG stars, because they have been discussed by many authors (e.g., Fenner et al. 2004; Bekki et al. 2007; D'Ercole et al. 2010). Since the numerical methods for the dynamical evolution of dwarfs with GCs in the Galaxy were already given in BY12, we briefly describe them below. For clarity, we describe the one-zone chemical evolution models originally developed by T11 and the results of the models in a separate section, §4.

2.2. *Dwarf galaxy*

A GC-host dwarf galaxy is assumed to consist of a dark matter halo and a stellar disk without nucleus. Both the dark matter halo and the stellar disk of the dwarf are represented by collisionless N-body particles. Gas dynamics, star formation, chemical evolution, and dust formation are not included at all in the present study (i.e., the simulations are purely collisionless ones). The dark matter halo with with the total mass of $M_{\rm h}$ is represented by the 'NFW' one (Navarro et al. 1996) with a central cusp predicted by the Cold Dark Matter (CDM) model:

$$\rho(r) = \frac{\rho_0}{(r/r_{\rm s})(1+r/r_{\rm s})^2}, \quad (1)$$

where r, ρ_0, and $r_{\rm s}$ are the distance from the center of the cluster, the central density, and the scale-length of the dark halo, respectively. The virial radius ($r_{\rm vir}$), the scale radius ($r_{\rm s}$), and the 'c' parameter ($=r_{\rm vir}/r_{\rm s}$) are chosen such that the values are consistent with recent cosmological simulations for the adopted $M_{\rm h}$ (Neto et al. 2007).

For comparison, we also investigate the models with 'cored dark matter' halos (Salucci & Burkert 2000; 'SB' profile), the density profile of which is described as follows:

$$\rho(r) = \frac{\rho_{0,\rm dm}}{(r + a_{\rm dm})(r^2 + {a_{\rm dm}}^2)}, \quad (2)$$

where $\rho_{0,\rm dm}$ and $a_{\rm dm}$ are the central dark matter density multiplied by $a_{\rm dm}^3$ and the core (scale) radius, respectively. Bekki et al. (2003) already demonstrated that dwarf galaxies with SB profiles are more susceptible to tidal destruction by larger and more massive halos than those with NFW profiles and discussed the transformation of nucleated dwarfs into naked nuclei. Therefore, we do not discuss much about dwarf destruction processes for dwarfs with SB profiles and GC evolution within them. We show the results for only one model with $M_{\rm h} = 10^{10} M_\odot$, $a_{\rm dm} = 0.92$ kpc, and $r_{\rm vir} = 9.2$ kpc.

The dwarf is assumed to be as a bulge-less disk galaxy with the total stellar mass of $M_{\rm s}$ and the size of $R_{\rm s}$. The radial (R) and vertical (Z) density profiles of the stellar disk are assumed to be proportional to $\exp(-R/R_0)$ with scale length $R_0 = 0.2R_{\rm s}$ and to $\mathrm{sech}^2(Z/Z_0)$ with scale length $Z_0 = 0.04R_{\rm s}$, respectively. In addition to the rotational velocity caused by the gravitational field of disk and dark halo components, the initial radial and azimuthal velocity dispersions are assigned to the disc component according to the epicyclic theory with Toomre's parameter $Q = 1.5$. The vertical velocity dispersion at a given radius is set to be 0.5 times as large as the radial velocity dispersion at that point. The stellar disk is assumed to have no stellar nucleus initially, which is different from the initial disk model adopted by BY12.

2.3. *GCs*

A dwarf galaxy is assumed to have two GCs located in different regions within the dwarf. Two GCs are denoted GC1 and GC2 for convenience, and they are represented by collisionless particles. GC1 and GC2 have different total mass ($m_{\rm gc,1}$ and $m_{\rm gc,2}$, respectively) and distances ($R_{\rm gc,1}$ and $R_{\rm gc,2}$, respectively). For convenience, the larger GC is referred to as GC1 in the present study. Recent theoretical studies of GC formation have shown that new stars can be formed from gas ejecta from AGB stars of GCs (D08, B11). The new stars and the existing stars are often referred to 'SG' and 'FG' stars, respectively, and we adopt these abbreviations in the present paper. The SG systems are demonstrated by these previous works to be more compact than the FG ones, because SG stars can form in the deep potential wells of FG stellar systems. Following these results, we mainly investigate 'two-component' GC models in which a GC is composed of FG and SG systems with different masses (e.g., $m_{\rm FG,1}$ and $m_{\rm SG,1}$ for GC 1) and sizes ($r_{\rm FG,1}$ and $r_{\rm SG,1}$ for GC1). For comparison, we also investigate 'one-component' GC models in which a GC is composed only of a FG system.

Each sub-population (FG or SG) in a GC is assumed to have the radial density profiles of stars described by a Plummer model with the scale length (a) being 0.2 times the size of the stellar system (e.g., $a_{\rm FG,1} = 0.2r_{\rm FG,1}$). Each cluster has 3D velocities that are the same as those of its nearest star in the stellar disk of the GC-host dwarf. The mass-ratio of two GCs ($m_2 = M_{\rm gc,2}/M_{\rm gc,1}$, where $M_{\rm gc,1}$ is always larger than or equal to $M_{\rm gc,2}$) is one of the most important parameters that can determine whether the GCs can merge with each other before the complete destruction of their host dwarfs. We mainly investigate the models in which $m_{\rm FG,1} = m_{\rm FG,2}$ (i.e., major GC merging), because BY12 have shown that major merging is more likely to occur than minor merging with $m_{\rm FG,1}/m_{\rm FG,2} < 0.3$ within dwarfs.

Vesperini et al. (2013) investigated the dynamical evolution of GCs with FG and SG stars that have initially different spatial distributions using N-body simulations. They found that complete spatial mixing of the two stellar populations due to two-body relaxation is possibly only in the advanced stage of dynamical evolution. We do not discuss the two-body relaxation effects on the evolution of merged GCs with initially two populations in the present study, though it is a quite interesting issue. Recently Ganagnin et al. (2016) have extensively investigated the structure and kinematics of the remnant of GC mergers for a wide range of densities and mass-ratios of merging GCs. Although these results are quite useful for understanding the origin of rotation in GCs (e.g., Anderson & King 2003; Bekki 2010a), we do not conduct such an extensive study of structural and kinematical properties of merged GCs, because our main interest is the probability of GC merging.

2.4. *Dwarf orbit and the gravitational potential of the Galaxy*

We mainly investigated two models, 'the present' and 'young' Galaxy (Milky Way; MW) models to discuss the GC merging and stripping in early and late phases of the Galaxy evolution. The model parameters for halo, bulge, and disk components of the Galaxy are different between the present and young MW models. The Galaxy in present MW models is assumed to have a *fixed* three-component gravitational potential and the orbit of the dwarf can be determined by the details of the potential for given its initial 3D positions, (x, y, z), and 3D velocities, ($v_{\rm x}$,$v_{\rm y}$,$v_{\rm z}$), with respect to the Galactic center. The following logarithmic dark matter halo potential is adopted for the Galaxy,

$$\Phi_{\rm halo} = v_{\rm halo}^2 \ln(r^2 + d^2), \quad (3)$$

where $d = 12$ kpc, $v_{\rm halo} = 131.5$ km s^{-1} and r is the distance from the center of the Galaxy. The gravitational potential of the Galactic disk is represented by a Miyamoto-Nagai (1975) potential;

$$\Phi_{\rm disk} = -\frac{GM_{\rm disk}}{\sqrt{R^2 + \left(a + \sqrt{z^2 + b^2}\right)^2}}, \quad (4)$$

where $M_{\rm disk} = 1.0 \times 10^{11}\ M_\odot$, and $a = 6.5$ kpc, $b = 0.26$ kpc, and $R = \sqrt{x^2 + y^2}$. The following spherical Hernquist (1990) model is adopted for the potential of the Galactic bulge;

$$\Phi_{\rm bulge} = -\frac{GM_{\rm bulge}}{r + c}, \quad (5)$$

where $M_{\rm bulge} = 3.4 \times 10^{10}\ M_\odot$, and $c = 0.7$ kpc. This reasonable set of parameters gives a realistic rotation curve for the Galaxy with a maximum rotation speed of 224 km s^{-1} at $R = 8.5$ kpc.

For the young MW models, the above three potential profiles with different parameters for the total masses of the three components are adopted: $M_{\rm disk} = 1.0 \times 10^{10}$

$M_\odot$, $M_{\rm bulge} = 3.4 \times 10^9$ $M_\odot$, and $v_{\rm halo} = 93.0$ km s^{-1}. This combination of parameters is chosen to mimic the young MW (at the time of major GC formation) with a possibly much lower mass and thus a lower maximum circular velocity. The epoch of dwarf accretion onto the Galaxy can be quite different between different dwarfs with GCs and the Galactic potential should be time-evolving owing to hierarchical mass accretion. By using the two extreme cases of the Galactic gravitational potential, we try to understand how the Galactic tidal field can influence GC merging during dwarf destruction.

The 3D position of the Galactic center is fixed at (x,y,z) = (0,0,0) whereas the initial 3D position and velocity of a dwarf galaxy are free parameters that can determine the orbital evolution of the dwarf around the Galaxy. The three basic parameters are (i) the initial distance of the dwarf from the Galactic center ($R_{\rm i}$), (ii) the initial velocity $f_{\rm v} v_{\rm c}$, where $v_{\rm c}$ is the circular velocity at $R_{\rm i}$ and $f_{\rm v}$ is a parameter that controls the orbital eccentricity and ranges from 0.1 (highly eccentric orbit) to 1 (circular orbit). and (iii) the inclination angle between the Galactic disk plane (=the x-z plane) and the orbital plane of the dwarf (θ). The initial x-component of the velocity of the dwarf is set to be 0, which means that $R_{\rm i}$ corresponds to the apocenter distance of the dwarf's orbit, because $f_{\rm v}$ is always less than 1. We mainly investigate the model ('standard orbit', defined as 'O1') in which $R_{\rm i}$=17.5 kpc, $f_{\rm v} = 0.5$, and $\theta = 45°$, because dwarf galaxies can be destroyed almost completely within ~ 3 Gyr in this model. We also investigate models with different $R_{\rm i}$, $f_{\rm v}$, and θ in order to investigate how the details of the orbital evolution of dwarfs can influence the merging processes of GCs. The initial angle between the stellar disk of a dwarf and the orbital plane of the dwarf is 60 degrees for all models in the present study.

2.5. *Parameter study*

Although we investigated numerous models (56 models), we present the results of 19 representative models, for which the model parameters are described in Table 1. The model parameters for 6 dwarf galaxy models investigated in the present study (D1-D6) and the adopted orbits of the dwarfs (O1-O4) are summarized in Table 2 and 3, respectively. Two GCs are assumed to exist initially in a simulated dwarf, because we think that the time delay between the formation epochs does not influence their evolution within the dwarf. We mainly show the results of the fiducial model (M1) with the dwarf galaxy model D1 ($M_{\rm h} = 10^{10}$ M$_\odot$) $m_{\rm FG,1} = 10^6 M_\odot$, $a_{\rm FG,1} = 10$ pc, $m_2 = 1$ (the mass-ratio of two GCs), $R_{\rm gc,1} = 100$ pc, $R_{\rm gc,2} = 200$ pc, and the standard orbit model O1, because it clearly shows a typical behavior of GC merging in a massive dwarf galaxy being destroyed by the Galaxy. We mainly focus on the possibility and timescale of GC merging in dwarf galaxies and their dependency on model parameters such as $M_{\rm h}$ and $m_{\rm FG.1}$. The timescale of GC merging ($t_{\rm merge}$) for each model is given in Table 1. We define $t_{\rm merge}$ as the time when (i) the separation of two GCs becomes less than 10pc and (ii) the separation becomes the minimum for the first time. The above condition (i) is necessary, because some models do not show GC merging. We also investigate the fraction of SG stars in the halo regions around merged GCs in order to discuss the observed physical properties of stellar halos around GCs (e.g., Olszewski et al. 2009). GC merging process can be influenced by the presence of stellar galactic nuclei, however, we do not discuss this possible important effect in the present study. Appendix A discusses briefly this issues using a few models with stellar galactic nuclei.

We investigate the evolution of dwarfs with GCs over 2.82 Gyr and 5.64 Gyr for the models with smaller $R_{\rm i}$ (=8.5 and 17.5 kpc) larger initial $R_{\rm i}$ (35 kpc), respectively. We run a low-mass dwarf model ($M_{\rm h} = 10^8 M_\odot$) without GCs (M19) in order to show the orbit of a dwarf that is not influenced by GCs (e.g., dynamical friction) and stripped field stars for a given gravitational potential: a dwarf's orbit defined by the time evolution of the position of the central star can be slightly influenced by massive GCs and stripped stars. GCs can continue to lose a significant fraction ($\sim 60\%$) of their stars through two-body relaxation and tidal stripping by the Galactic tidal field over the time scale of ~ 10 Gyr (e.g., Vesperini 1997; Vesperini et al. 2011). These long-term effects are not properly included, because we run simulations for only $3-6$ Gyr. Accordingly, the final masses of GCs could be larger than the observed ones in the present study. For example, if the present-day mass of M22 is $2.9 \times 10^5 M_\odot$ (e.g., Marks & Kroupa 2010), then its mass before losing stars through the above long-term dynamical effects should be at least $4.8 \times 10^5 M_\odot$. The initial mass of M22 at its birth could be even by a factor of $5-10$ larger than this $4.8 \times 10^5 M_\odot$, because FG stars can be lost during the early evolution of GCs (e.g., D'Ercole et al. 2008).

2.6. *Simulation set up*

We use a newly revised, more sophisticated version of our original simulation code adopted in BY12 so that we can investigate not only global dynamical evolution of dwarf galaxies influenced by the Galactic tidal field but also the orbital evolution of GCs within them. The time integration of the equation of motion is performed by using 2nd-order leap-flog method with the maximum time step interval being 1.41×10^6 yr for particles in a dwarf galaxy and 2.82×10^4 yr for particles representing GCs. The adopted individual time step scheme with rather small time step interval for GC stars enables the present study to investigate GC merging more properly than BY12, because such scheme was not introduced by BY12.

The total number of particles for dark matter, stellar disk, GC of a dwarf galaxy is 500,000, 500,000, and 60,000, respectively. The FG and SG systems are represented by 20000 and 10000 collisionless particles in all models. Only a limited amount of computations time is allocated for the research project on which the present study is based and we need to run at least ~ 60 models with different model parameters in the present investigation. We therefore consider that the total number particle of $\sim 10^6$ is reasonable (not numerically costly) that we can adopt for each model. The gravitational softening lengths (ϵ) for dark matter halo, stellar disk, FG system, and SG system (of a GC) are denoted as $\epsilon_{\rm dm}$, $\epsilon_{\rm s}$, $\epsilon_{\rm FG}$, and $\epsilon_{\rm SG}$, respectively. We determine ϵ for each of these components based on the half-number radius of the particles. We consider that when two different components interact gravitation-

ally, the mean softening length for the two components is applied for the gravitational calculation. For example, $\epsilon = (\epsilon_{\rm dm} + \epsilon_{\rm s})/2$ is used for gravitational interaction between dark matter particles and stellar ones in a dwarf. In the fiducial model, $\epsilon_{\rm dm}$, $\epsilon_{\rm s}$ $\epsilon_{\rm FG}$, and $\epsilon_{\rm SG}$ are set to be 104 pc, 10.8 pc, 0.93 pc, and 0.37 pc, respectively, in the fiducial model (M1). In the following, T in a simulation represents the time that has elapsed since the simulation started.

3. RESULTS: GC MERGING

3.1. *The fiducial model*

Figure 3 shows how the spatial distributions of field stars of a dwarf disk galaxy and stars from FG and SG systems in two GCs evolve with time during the accretion of the dwarf onto the Galaxy in the fiducial model M1. This model corresponds to a later accretion of a dwarf onto the present Galaxy so that the strong tidal field of the Galaxy can rapidly destroy the dwarf within ~ 3 Gyr. A significant fraction of FG stars can be efficiently stripped from GC1 and GC2 by the dwarf's tidal field while the two GCs are orbiting around the host dwarf ($T = 0.56$ Gyr). These stripped FG stars spread over the entire disk region of the dwarf ($T = 1.12$ Gyr) and then are stripped from the dwarf while the stellar disk component of the dwarf is being destroyed by the Galactic tidal field ($T = 1.68$ and 2.24 Gyr). After the complete destruction of the dwarf by the Galactic tidal field, the new GC (or naked nucleus) can continue to lose their FG and SG stars with FG stars being more efficiently stripped by the tidal field. Clearly a tidal stream connecting with the halo of the new GC can be seen at $T = 2.24$ Gyr, whereas there is no such connection at $T = 2.82$ Gyr. The final total mass of GC stars at $T = 2.82$ Gyr is $6.2 \times 10^5 M_\odot$ for $R \leq 10$ pc and $1.2 \times 10^6 M_\odot$ for $R \leq 50$ pc.

Since the dynamical friction of GCs against disk field stars of the dwarf is quite effective owing to the lower velocity dispersion of field stars (Bekki 2010b), the two GCs can spiral into the central region of the dwarf and finally merge with each other. As shown in Figure 4, the two GCs can rather quickly merge to form a new GCs (a single nuclear GC) at $T \sim 0.32$ Gyr. The SG systems do not lose a significant fraction of stars during major GC merging so that the new SG system can be still more compact. A significant fraction of the FG stars can be stripped to form a stellar halo during GC merging. The final remnant of GC merging can have diffuse FG and compact SG system, and the remnant can still have a nested structure ($T = 1.12$ Gyr). The stellar halo around the new GC is quite extended within its host dwarf and the halo is dominated by FG stars at $T = 0.56$ Gyr when the new GC can be identified as an off-center nucleus. Thus, this fiducial model demonstrates how two massive GCs with FG and SG stars can be transformed into one new GC with four distinct stellar populations (i.e., original FG and SG stars from GC1 and GC 2) during the destruction of their host galaxies.

Figure 5 shows how the mass fractions of disk field stars of the dwarf ($F_{\rm Field}$) depends on the distance (R) from the center of the remnant of GC merging. The mass fraction is not so large ($< 3\%$) in the halo region of the new GC ($R < 50$ pc; original radius of the FG system) at $T = 2.82$ Gyr, which means that the field stars can not be tidally captured by the merged GC so efficiently in this model. These stars that are gravitationally trapped within the merged GC (i.e., those with their velocities less than the escape velocity of the GC) are mostly from the inner regions of the dwarf. Both dwarf galaxies and the Galaxy are observed to have negative metallicity gradient (e.g., Andrievsky et al. 2004; Tolstoy et al. 2004 de Boer et al. 2012), though these dwarfs with examined metallicity gradients are dwarf spheroids rather than dwarf disks (irregulars). Hidalgo-Gamez et al. (2010) revealed negative abundance gradients in [Fe/H] and oxygen with ~ -0.2 dex kpc^{-1} in dwarf spirals, though their paper is yet to be published. Given these observations, the trapped stars can be possibly more metal-rich in some dwarf disk galaxies. The derived small fraction of field stars around the new GC is consistent with the previous results by BY12.

A significant contribution of field stars ($\sim 20\%$) to the halo region of the GC can be seen only in the very outer part of the new GC ($R \sim 100$ pc), though not all of these outer halos stars are gravitationally bound to the new GC. The mass fraction of SG stars within the central 10pc of the new GC ($\sim 60\%$) is consistent with the observed fraction of SG stars (e.g., Carretta et al. 2009). A much smaller fraction of stars can be stripped from the SG system of the new GCs so that the halo of the new cluster can not be dominated by the stripped SG stars (at most $\sim 20\%$). The presence of SG stars in the simulated GC is not so consistent with recent observations which have not yet discovered the presence of SG stars in the halos of examined GCs (e.g., NGC 1851; Marino et al. 2015). However, the lack of SG stars in these GCs could be simple due to the expected small number of SG stars in the halo regions.

Figure 5 shows the separate rotation curves ($V(R)$) of the FG and SG systems of the new GC at $T = 2.82$ Gyr. The $V(R)$ profiles along the y-axis are derived using the x-components of line-of-sight velocities for stars within 50pc from the GC center are used at each radial bin. Both FG and SG stars are being stripped at $T = 2.82$ Gyr, and therefore the stars connecting to the tidal streams introduce a larger velocity dispersion. The global rotation of the GC can be seen slightly more clearly in the SG system than in the FG, though the rotation amplitude is small (~ 1.5 km s^{-1}) for FG and SG stars. There is little rotation in the central 10 pc both for the FG and SG stellar systems. Although the amplitude of rotation of merged GCs depends on the viewing angles and the orbits of merging GCs, it is quite small (at most 5 km s^{-1} in different projections).

3.2. *Parameter dependence*

It is found that the total masses of GCs, the initial positions of GCs within their host dwarfs, and the physical properties of GC hosts, and the orbits of GC hosts can determine the probability of GC merging. These results, some of which are essentially the same as those reported in BY12, are summarized as follows.

(1) Figure 6 shows that if both GCs have $r_{\rm gc} \leq 600$ pc, then the two GCs can merge with each other well before the complete destruction of their host in the dwarf model

D1 (See M2 and M3). Such GC merging within their host can not occur in the model M4 in which one of the two GCs is initially located in the outer part of the host ($R = 800$ pc). This results can be understood as follows. The timescale of a GC to spiral in the nuclear regions of its host dwarf due to dynamical friction is longer for larger $r_{\rm gc}$, and GCs with larger $r_{\rm gc}$ are more likely to be stripped from their host dwarf during the tidal interaction between the dwarf and the Galaxy. Therefore, only GCs initially in the central regions are expected to merge with one another before they are tidally stripped from their hosts.

(2) GC merging is unlikely within ~ 2 Gyr (=timescale of dwarf destruction; $t_{\rm dest}$) in the model M5 with $m_{\rm FG,1} = 3 \times 10^5 M_\odot$ and in the model M6 with $m_{\rm FG,1} = 10^5 M_\odot$, as shown in Figure 6. These results suggest that there could be a threshold GC mass above which GC merging is possible in dwarfs. These results also imply that more massive GCs (e.g., M22) are more likely to become GCs with metallicity spreads though GC merging, because GCs formed in different local regions within their dwarfs at different times are likely to have different metallicities.

(3) If the mass-ratio of two GCs is low ($m_2 = 0.1$), then GC merging within $t_{\rm dest}$ is not possible even for $m_{\rm FG,1} = 10^6 M_\odot$, as shown for the model M7 in Figure 6. This is because the timescale of dynamical friction for the smaller GC is quite long: the two GCs can not become close enough to merge in the central region of their host dwarf. This result implies that the mass ratios of two populations with different metallicities in a GC does not differ so much, if GCs with metallicity spreads are formed from GC merging. The mass-ratios of two populations with different [Fe/H] in anomalous GCs such as NGC 1851 and M22 have not been precisely determined or clearly documented yet (e.g., Marino et al. 2011). The present simulations predict that the mass-ratios of two populations with different [Fe/H] should be comparable in anomalous GCs.

(4) If GC-host dwarf galaxies are as massive as $M_{\rm h} = 3 \times 10^{10} M_\odot$ (corresponding to the Magellanic Clouds), then GC merging becomes less likely even for massive GCs with $m_{\rm FG,1} = 10^6 M_\odot$. This is mainly because dynamical friction time scale is longer in more massive dwarfs for a given GC mass: if the relative velocity between the GC and the field stars is larger (as is the case for more massive dwarfs), then the dynamical friction time scale is longer. The model M11 with the massive dwarf model D4 ($M_{\rm h} = 3 \times 10^{10} M_\odot$) do not show GC merging if two GCs are located at $R = 100 \sim 200$ pc. This result suggests that formation of anomalous GCs through GC merging is possible in dwarfs that are not too massive. It is confirmed that major merging of two GCs with with $m_{\rm FG,1} = 3 \times 10^6 M_\odot$ is possible in very massive dwarfs with $M_{\rm h} = 3 \times 10^{10} M_\odot$, though the GC merger remnant is quite massive (like ω Cen). This indicates that the mass-ratios of GCs to dark matter halos ($f_{\rm m,gc}$) is a key parameter for GC merging.

(5) It is confirmed that the probability of GC merging does not depend on whether or not GCs are composed only of FG stars or both of FG and SG stars: The model M12 with only FG stars demonstrates GC merging within less than 1 Gyr. Also, the models M14, M15, and M16 show that GC merging is possible in the young Galaxy model, which strongly suggests that the formation of anomalous GCs through GC merging within dwarf is possible in the early formation history of the Galaxy. Although the timescale of GC merging becomes longer for larger initial distances of dwarfs (e.g., M18 for O2 orbit), GC merging process itself is not strongly influenced by the initial distances of GC host dwarfs. The dark matter density profiles of dwarfs do not influence GC merging so greatly, if GC masses are large enough ($m_{\rm FG,1} = 10^6 M_\odot$), as shown in the model M17.

(6) Figure 7 shows that the mass fractions of field stars in the halos of merged GCs does not depend so much on model parameters ($F_{\rm field} \sim 0.1$). The presence of field stars within 10-20 pc of merged GCs can be seen only if the initial masses of individual GCs to their hosts ($f_{\rm m,gc}$) are higher ($f_{\rm m,gc} \sim 0.0001$). Since the field stars finally within merged GCs are mostly from the inner region of dwarfs, field stars within the GCs (i.e., anomalous GCs) are likely to be observed as anomalous metal-rich stars. GC1 in the model M4 in which GC merging is not possible have no field stars in the outer part, because the GC is tidally stripped from the host dwarf so that it can have little time to tidally capture field stars. This results suggests that GC merging is essential to host field stars in the halo regions of GCs. The merged GC in the model M9 has a large mass ratio of field stars to FG stars in its halo, because the destruction of its host dwarf has just been complete at $T = 2.8$ Gyr and therefore disk field stars can still remain in the surrounding region of the GC. This result means that anomalous GCs just after their 'release' from the host dwarfs can have large halos dominated by field stars.

(7) The dwarf galaxy in the model M13 without GCs can not be completely destroyed by the Galaxy within ~ 3 Gyr, which is in striking contrast with the fiducial model with GCs which shows complete tidal destruction of the dwarf galaxy within 2 Gyr. This result implies that spiral-in of GCs can lower the central density of the dark matter halo of its host dwarf so that the dwarf becomes more susceptible to tidal destruction after GC merging. This role of GC merging in the destruction process of GC host dwarf is a preliminary result and will need to be re-investigated more extensively in our future studies.

(8) The present results do not depend strongly on the models of the Galaxy, the central densities of dark matter halos of dwarfs, and the orbits of th dwarfs. For example, as shown in Table 1 for M14 - M16, merging of more massive GCs in dwarfs is possible for the young Galaxy model. Also, GC merging is possible in the cored dark matter model, M17, and in M18 in which the apocenter of the dwarf orbit is twice as large as that in the fiducial model. These results demonstrate that merging of two massive GCs is possible in massive dwarfs being destroyed by the Galaxy and thus that anomalous GCs can originate from such massive dwarfs.

4. LINKING CHEMICAL EVOLUTION OF DWARFS WITH CHEMICAL ABUNDANCES OF GCS

4.1. *One-zone models*

To validate the theoretical interpretation presented in the previous sections, we calculate the evolution of Ba (a *s*-process element), Eu (a *r*-process one), and Fe abundances for dwarf galaxies with different star formation histories. The chemical evolution model which we adopt here is essentially the same as those constructed for the Fornax dSph galaxy in T11. Although the star formation histories of host dwarf galaxies for the Galactic GCs can be quite diverse, we focus mostly on the host for M22. We slightly modify only two parameters (i.e., star formation rate, SFR, and stellar initial mass function) in the models by T11 so as to be in better agreement with the chemical feature of the host dwarf galaxy for M 22. Since the details of the model is given in T11, we just briefly describe the essence of the models below.

The basis for the model is that a dwarf galaxy is formed through a continuous infall of almost pristine gas ([Fe/H]$=-5$) from outside. With this framework, the star formation rate (SFR) at a time step t is assumed to be proportional to the gas fraction with a constant rate coefficient ν Here, ν is the fraction of the gas mass that is converted into stars per Gyr. For the infall rate, we apply a formula that is proportional to $\exp(-t/\tau_{\rm in})$ with a timescale of infall of $\tau_{\rm in}$. For the best model, the values of (ν, $\tau_{\rm in}$)=(1.0, 0.1) are assigned. The initial mass function (IMF) is assumed to be a power-law mass spectrum with a slope of -1.35, i.e., a canonical Salpeter IMF, with a fixed lower mass cutoff of $0.05M_{\odot}$ and a variable upper mass cutoff of $m_{\rm upp}$. The *r*-process yield from a neutron star merger is assumed as follows. We adopt the ejecta mass of a neutron star merger is 0.01 $Modot$. Since the frequency of neutron star mergers is estimated to be one per a few 1000 SNe II (Tsujimoto & Shigeyama 2014), we determine its frequency within the possible range so as to be the nucleosynthetic [Eu/Fe] ratio of +0.5 as observed in M22 or Galactic halo stars, where the Fe yield is the average from an SN II: In this case, the predicted (calculated) [Eu/Fe] exactly becomes +0.5. A delay time of ejection from a neutron star merger is assumed to be 10^7 yrs. The details of nucleosynthesis yields for Ba and light elements (C, N, and O) adopted in the present study are given in T11 and Tsujimoto & Bekki (2011), respectively.

As in the case for the Fornax, we find that a small $m_{\rm upp}$ of $25M_{\odot}$ is the best solution to obtain a high [Ba/Fe] ratio within a short timescale ($<$ 1 Gyr). Therefore we mainly discuss the results of the best model with (ν, $\tau_{\rm in}$, $m_{\rm upp}$)=(1.0, 0.1, 25) (referred to also as 'high SFR and low $m_{\rm upp}$' model) in the present study. We do not consider the contribution from Type Ia SNe (SNe Ia) since no signature of chemical enrichment by SNe Ia is seen in the ratio of α-elements to Fe for the two populations of M22. This assumption seems incompatible with the delay time distribution of SNe Ia obtained from the studies on the SN Ia rate in distant and nearby galaxies, which claim that SNe Ia start from a $\sim 10^8$ yrs delay from the initial star formation (e.g., Maoz et al. 2011). However, for instance, the Sagittarius dSph galaxy which is as massive as a candidate for the progenitor of M22, exhibits no signature of chemical enrichment by SNe Ia until [Fe/H]~ -1.3 (de Boer et al. 2014a), where about 1-3 Gyr is implied to elapse after the start of star formation from the age-metallicity relation (McWilliam et al. 2013; de Boer et al. 2014b). In addition to the best case, we show another two cases of (ν, $\tau_{\rm in}$, $m_{\rm upp}$)=(0.3, 0.1, 25) ('low SFR and low $m_{\rm upp}$' model) and (1.0, 0.1, 50) ('high SFR and high $m_{\rm upp}$' model) to demonstrate the dependence of the results on the adopted parameters. Here we just see the early evolution of a dwarf galaxy for the duration of star formation of 1 Gyr, which is compatible with the observed old ages of the Galactic GCs (e.g., M22).

4.2. *Results*

Figure 8 shows the results for the best model corresponding to the host dwarf of M22 and other two comparative ones. The best model denoted by the red solid line broadly reproduces the correlation of [Ba/Fe] and [Fe/H] corresponding to the two populations of M22 with a short timescale of a few 10^8 yrs. Comparison of this model result with that for the model with a high $m_{\rm upp}$ of $50M_{\odot}$ (black dot-dashed line) reveals that an efficient Ba enrichment in comparison with Fe enrichment is realized by introducing a small $m_{\rm upp}$. It is attributed to the result that a small $m_{\rm upp}$ yields a reduction in the Fe mass ejected from each generation of SNe II, whereas the amounts of s-process elements synthesized in low-mass AGB stars remain unchanged. It should be noted here that the time evolution of [Ba/Fe] is rather rapid (i.e., steeper age-dependence of [Ba/Fe]) for ages less than 0.5 Gyr and then it becomes less rapid (i.e., flatter [Ba/Fe]-age relation). This might have some constraints on the formation epochs of two GCs that finally merge with other to form a single anomalous GC in dwarfs: larger [Ba/Fe] differences in earlier formation of anomalous GCs via merging.

As shown in the upper panel of Figure 8, the model with low SFR and low $m_{\rm upp}$ (blue short-dashed line) has an almost same trend of [Ba/Fe] evolution as obtained for the best model, which suggests that the rapidity of SF does not much influence the evolution of [Ba/Fe] in dwarf galaxies. However, this model with low SFR shows (i) a rather low [Fe/H] that is not consistent with [Fe/H] of metal-poor GCs ([Fe/H]~ -1.6) and (ii) a very slow [Fe/H] evolution that can not cause a significant [Fe/H] difference of ~ 0.2 dex after 0.3 Gyr, as required for the case of the host of M22. These results of three models therefore clearly demonstrate that both high SFR and lower $m_{\rm upp}$ are required for explaining both the increase of [Ba/Fe] by ~ 0.3 dex and that of [Fe/H] by ~ 0.15 dex within ~ 0.3 Gyr chemical evolution of dwarf galaxies. It it our future work to investigate how such a rapid SF with lower $m_{\rm upp}$ is possible for GC-host dwarf galaxies.

The upper panel of Figure 9 shows the time evolution of [Eu/Fe] for the best model, which is assumed to be "massive" dwarf galaxies such as the Fornax dwarf spheroidal galaxy (see §5.3 for the discussion on how the results depend on the stellar masses). In this model, mergers between neutron stars ('NS-NS merger') can occur so that [Eu/Fe] can be kept constant (e.g., Tsujimoto & Shigeyama 2014). However, the evolution of [Eu/Fe] in low-mass dwarf galaxy models can not be constant as this best model, because NS-NS merger is an extremely rare

event (i.e., almost no NS-NS mergers, which end up with a decreasing trend of [Eu/Fe] with [Fe/H]). The lower panel of Figure 9 shows that the time evolution of [Ba/Eu] is very similar to that of [Ba/Fe] in Figure 8, which is totally expected for a flat evolution of [Eu/Fe] in massive dwarf galaxies (Tsujimoto & Shigeyama 2014). These results in Figure 9 suggest that [Eu/Fe] and [Ba/Eu] of GCs have fossil information of the chemical evolution of their host dwarfs.

Although the present one-zone chemical evolution model can reproduce the observed [Ba/Fe] difference in the two populations of M22 reasonably well, it can not simply explain the observed difference in [(C+N+O)/Fe] in the two populations (Fig. 17 in Marino et al. 2011). Figure 10 shows that an enhancement of [C/Fe] by 0.1 dex is possible between ages of 0.2 and 0.8 Gyr in the best model (indicated by the red solid line). Figure 10, however, shows that [(C+N+O)/Fe] can not become enhanced by +0.1 dex within 1 Gyr in the three models, which means that the present model fails to reproduce both [Ba/Fe] and [(C+N+O)/Fe] spreads observed in M22 self-consistently. Mixing of ISM with ejecta from AGB stars and SNe is assumed in the present model so that [(C+N+O)/Fe] can not be rapidly enhanced (within 300-500 Myr). Such a large difference in [(C+N+O)/Fe] between the two populations might be possible, if new stars can form from gaseous ejecta from AGB stars without mixing so well with ISM. We will investigate this issue in our future studies using new chemical evolution models that can freely change the mass fraction of ISM mixing with AGB ejecta.

5. DISCUSSION

5.1. *What distinguishes between normal and anomalous GCs ?*

The present study has demonstrated that GCs with internal metallicity spreads can be formed from merging of at least two GCs within their host dwarf galaxies before the complete destruction of the hosts by the Galactic tidal field. In this merging scenario of anomalous GC formation, less massive two GCs can not merge with each other quickly within dwarfs so that they can not have internal metallicity spreads. Although such less massive GCs can have FG and SG populations with anti-correlations between light elements through self-enrichment processes, they are much more likely to be stripped from their hosts by the strong tidal field of the Galaxy. Thus, the initial total mass of a GC can be one of parameters that determine whether the GC can become an anomalous GC with internal metallicity spreads or normal GCs in this GC merging scenario.

Most of the Galactic anomalous GCs are observed to show abundance spreads in *s*-process elements and each of the *s*-poor and *s*-rich sub-populations have its own C-N and O-Na anti-correlations (s-Fe-anomalous GCs; Marino et al. 2015). In the GC merger scenario, self-enrichment of intra-cluster gas by AGB stars can proceed independently in each of two GCs formed in different places with a time lag between two GC formation events ($t_{\rm lag}$). Therefore, if merging of two GCs can occur at least $\sim$ 300 Myr after the younger of the two was formed (i.e., $t_{\rm merge} > t_{\rm lag}$+300 Myr, where 300 Myr corresponds roughly to the timescale of self-enrichment), then the new GC formed from GC merging can naturally become s-Fe-anomalous GCs. It has long been suggested that self-enrichment of intra-cluster gas by Type II supernovae can cause internal metallicity variations in GCs, if the GCs are massive enough to retain the SNII ejecta (e.g., Baumgardt et al. 2008). In this in-situ self-enrichment scenario, self-enrichment both by SNII and AGB stars is possible in massive GCs, and accordingly, *s*-Fe-anomalous GCs can be formed. However it is not clear in this scenario how each of the *s*-rich and *s*-poor populations in anomalous GCs (e.g., M22) show anti-correlations between light elements abundances.

In the GC merging scenario, $t_{\rm lag}$ and the rapidity of star formation in GC host dwarf ($t_{\rm sf}$) are the two main parameters that control the degree of abundances spreads in [Fe/H] and *s*-process elements of anomalous GCs. If $t_{\rm lag}$ is shorter in a dwarf, then Δ[Fe/H] and Δ[Ba/Fe] of anomalous GCs are smaller for a given dwarf's SFH in this scenario. On the other hand, if a GC-host dwarf is forming stars slowly, then Δ[Fe/H] and Δ[Ba/Fe] in anomalous GCs formed in the dwarf can be small even for larger $t_{\rm lag}$. It should be noted here that $t_{\rm lag} < t_{\rm merge}$ and $t_{\rm sf} < t_{\rm merge}$ are required for the formation of s-Fe-anomalous GCs. It depends on the physical properties of GC-host dwarfs whether these two conditions can be met. The present results are based on purely collisionless simulations, which do not incorporate possible important effects of baryon physics on the orbital evolution of GCs in low-mass dwarfs, such as strong supernova feedback effects on ISM in low-mass dwarf embedded in massive dark matter halos (e.g., Maxwell et al. 2012). Since such bayonic effects can possibly influence $t_{\rm merge}$, $t_{\rm sf}$, and $t_{\rm lag}$, we will need to investigate whether both $t_{\rm lag} < t_{\rm merge}$ and $t_{\rm sf} < t_{\rm merge}$ are satisfied in some dwarf galaxies based on more sophisticated hydrodynamical simulations of dwarf galaxy formation.

5.2. *Where do metal-rich anomalous stars come from ?*

Johnson et al. (2015) have recently made a detailed analysis of chemical abundances of the Galactic GC NGC 6273 and found that NGC 6273 has at least two stellar populations with [Fe/H] ranging from -1.8 to -1.3. In addition to the two populations, the presence of a third metal-rich 'anomalous stars' that have chemical abundance patterns different from those of the two populations have been discovered in NGC 6273 (Johnson et al. 2015). Using multi-wavelength HST photometry and previous results of chemical abundance studies for M2, Milone et al. (2015) have also found a third population ('C' component; anomalous stars) that does not have sub-population with different abundances of light elements in M2. It is well known that the Galactic GC ω Cen has such metal-rich stars (e.g., Lee et al. 1999), which implies that the star formation history of the GC should be quite different from those of other normal GCs.

It is unclear how these anomalous stars were formed after the formation of other two major populations in these massive GCs. The present study has shown that if the mass-ratio of a GC to its host halo ($f_{\rm m,gc}$) is higher in a massive dwarf galaxy, then field stars in the central region of the dwarf can finally reside within the merger remnant of GCs after they are tidally captured by the remnant. The present study therefore suggest a new scenario

in which the observed metal-rich anomalous stars in NGC 6273, M2, and ω Cen are originally field stars in their GC host dwarf galaxies. The higher [Fe/H] of anomalous stars in these GCs can reflect the chemical enrichment processes of their host GCs after the formation of the GCs in this scenario: it is not due to a prolonged SF *within* the GCs. The gravitational capture of field stars by massive GCs are likely to occur in the central regions of dwarfs, where star formation can proceed very rapidly owing to possible high-gas densities. As shown in Figure 8 of this paper, [Fe/H] can change very rapidly by an order of magnitude within a timescale of ~ 0.3 Gyr, which is shorter than the timescale of GC merging. It is therefore possible that nuclear regions have already high [Fe/H] when GCs merge and consequently start to capture nuclear field stars. Therefore, the third populations in these GCs can be more metal-rich in this scenario. The metal-rich third population in NGC 6273 exhibits a low level of *s*-process, which suggests that in a central region of a dwarf galaxy, a rapid SF likely proceeds with a short timescale, resulting in r-process-dominant abundances.

The new scenario predicts that low-mass GCs, can not have metal-rich anomalous stars, because such low-mass GCs are more likely to be tidally stripped from their host dwarfs before they spiral-in the nuclear regions of their hosts. Given that GCs can not become anomalous GCs with internal metallicity spreads without GC merging, the new scenario suggest that only anomalous GCs can have metal-rich anomalous stars. Although three GCs have been observed to have anomalous stars so far, it is not observationally clear whether the presence or absence of anomalous stars depend on the degree of internal metallicity variations in GCs. The detailed theoretical predictions on the chemical abundances and dynamical properties (e.g., spatial distributions within GCs) of anomalous stars in anomalous GCs are still lacking so that we can not discuss whether the new scenario is really promising in explaining their fundamental properties in a fully self-consistent manner. More observational and theoretical studies are required for better understanding the origin of these unique stellar populations in GCs.

5.3. *GC hosts should be massive: A clue from Eu*

Marino et al. (2011) found that [Eu/Fe] in stars of the Galactic GC M22 do not depend on [Fe/H] for $-2.0 <$[Fe/H]< -1.6. The observed flat evolution of [Eu/Fe] is consistent with GC host dwarfs being as massive as the Fornax dwarf galaxy or the LMC as follows. The constant [Eu/Fe] with an increasing [Fe/H] means that the Eu abundance increases with an increasing Fe abundance. Such a continuous increase of r-process element is characteristic of the chemical evolution of massive galaxies with their stellar masses larger than $\sim 10^6 M_\odot$ such as the Fornax and the Sagitarrius dwarf galaxies (Tsujimoto & Shigeyama 2014). In contrast, faint dwarf galaxies such as the Draco galaxy exhibit a constant [Eu/H] of ~ -1.3 with no apparent increase in the Eu abundance over the metallicity range of $-2 <$[Fe/H]< -1. In other words, [Eu/Fe] decreases with an increasing [Fe/H] in faint dwarf galaxies.

These results for low-mass dwarfs imply that there are no Eu production events while more than 10^3 SNe II increase the Fe abundance in the ISM of the dwarfs. This level of rarity of Eu production is compatible with the frequency expected for neutron star mergers, which is estimated to be one per 1000-2000 SNe II (Tsujimoto & Shigeyama 2014). For instance, the Draco galaxy, the stellar mass of which is $\sim 3 \times 10^5 M_\odot$ (Martin et al. 2008) is likely to host ~ 1500 SNe II in total, assuming a canonical IMF. Thus it is no wonder that no neutron star merger has occurred in the Draco, which results in the observed decreasing [Eu/Fe] feature. On the other hand, the Fornax dwarf galaxy ($\sim 2 \times 10^7 M_\odot$) is predicted to host ~ 100 events of neutron star mergers over the whole evolution. It will yield a continuous Eu increase with time, which is equivalent to the constant [Eu/Fe] feature as observed. Therefore, the constant [Eu/Fe] feature is the compelling evidence that a host galaxy for M22 should be sufficiently massive to continuously host a rare event of r-process production.

5.4. *A possible unified scheme*

The present study suggests that there are at least five key physical parameters that control the formation processes and chemical abundances of GCs. The first parameter is the total mass ($M_{\rm h}$) of a GC-host dwarf galaxy which determines whether a GC can be formed from massive gas clouds in the dwarf. Only if $M_{\rm h}$ of a dwarf galaxy exceeds a threshold halo mass ($M_{\rm h,th}$), FG stellar systems massive enough to host SG stars can be formed in the dwarf, as recent numerical simulations have demonstrated (Bekki 2016). The second parameter is the total mass of a GC ($m_{\rm gc}$), which controls the self-enrichment process of intra-cluster gas in forming GCs. If $m_{\rm gc}$ is larger than a threshold GC mass ($m_{\rm gc,th}$), then gaseous ejecta from AGB stars or massive stars can be retained and mixed with pristine gas in the deep gravitational potential of the GC so that new stars can form from the chemically enriched gas. This threshold GC mass for the formation of SG stars has already been discussed by several authors (e.g., D08; B11; Conroy & Spergel 2011).

The third parameter is the timescale of GC merging ($t_{\rm merge}$) within GC-host dwarfs. If this $t_{\rm merge}$ is shorter than the destruction timescale of GC host dwarf ($t_{\rm dest}$) by the Galactic tidal field during dwarf accretion onto the Galaxy, then anomalous GCs with metallicity spreads can form from GC merging. If $t_{\rm merge}$ is longer than $t_{\rm dest}$, then GCs are stripped from their host dwarfs before GC merging and consequently become the Galactic 'normal' GCs. Since the dynamical friction process of GCs within dwarfs is a key determinant for $t_{\rm merge}$, $m_{\rm gc}$ and mass densities and kinematics of field stars can control $t_{\rm merge}$. More massive GCs are more likely to have shorter dynamical friction timescale so that they can become anomalous GCs.

The fourth parameter is $t_{\rm dest}$, which can control the duration of star formation in dwarfs. Star formation can last longer in more massive dwarfs, because they are more likely to be disrupted by the Galactic tidal fields more slowly. If $t_{\rm dest}$ in a massive dwarf is as long as several Gyr, then chemical enrichment in the central region can lead to a very large [Fe/H] spread and a significant contribution of low-mass AGB stars to the evolution of *s*-process elements. The stellar nucleus or nuclear cluster in the dwarf can therefore show large abundance spread

in different elements (like ω Cen). The fifth parameter is $f_{\rm m,gc}$ (the mass-ratio of a GC to its host galaxy's dark matter halo), which controls the capability of merged GCs to capture field stars. GCs in dwarfs with higher $f_{\rm m,gc}$ are more likely to have field stars within them after GC merging, and these field stars are not initially in GCs and later captured by the GCs. These captured field stars may well be observed as anomalous metal-rich stars in anomalous GCs.

Figure 11 illustrates how the five parameters determine the levels of internal abundance spreads of GCs and Table 4 summarizes the physical meaning of the five parameters: this is just one of possible unified scenarios of GC formation. There are only five different classes of GCs in this illustration and only one proto-type of each GC class is shown just for clarity. In this scenario, the levels of internal abundance spreads in GCs depend not only on the physical properties of GCs ($m_{\rm gc}$) but also on the chemical and dynamical histories of their host GCs. This scenario is based on *separate* investigation of chemical and dynamical evolution of GCs and their host dwarfs, and accordingly they are not fully self-consistent. It is thus our future study to investigate how the chemical properties of GCs depend on their formation processes and the evolution of their host dwarfs using chemodynamical simulations of galaxy formation with a model for GC formation.

6. CONCLUSIONS

Using dynamical simulations of dwarf galaxies with GCs and chemical evolution models, we have investigated (i) merging processes of GCs in their host dwarf galaxies, (ii) stripping of GCs from their host dwarfs, (iii) tidal capture of field stars by merging GCs, (iv) final kinematics of merged GCs, and (v) various chemical abundances (e.g., [Fe/H] and [Ba/Fe]) of merged GCs. The present dynamical simulation is better than BY12 in that both GCs and their host dwarf galaxy are represented by N-body particles. Furthermore, the present study has considered that the chemical evolution of GC host dwarfs are linked to the internal abundance spreads of GC stars. The main results are summarized as follows.

(1) Merging between massive GCs with their masses ($M_{\rm gc}$) larger than 3×10^5 M$_\odot$ is inevitable in their host dwarf galaxies with $M_{\rm h}=[3\times10^9-3\times10^{10}]$ M$_\odot$ because of more efficient dynamical friction of the GCs against disk field stars in the host dwarfs. Given that the time scale of GC merging ($t_{\rm merge}$) is less than a few Gyr in these massive dwarfs, the merged GCs can become off-center nuclei before their hosts are completely destroyed by the Galactic tidal field. These results do not depend on whether GCs have both two generations (i.e., FG and SG) of stars or just single generation of stars.

(2) Low-mass GCs with $M_{\rm gc}\leq10^5$ M$_\odot$ can not lose their orbital energy and angular momentum efficiently so that they can not sink rapidly into the central regions of their hosts. Therefore they are more likely to be tidally stripped from their host dwarfs before GC merging to become 'normal' GCs (with C-N and Na-O anti-correlations). This result combined with the above result (1) strongly suggests that GC masses can distinguish between normal GCs and anomalous ones with [Fe/H] spreads. It has long been suggested that chemical enrichment of intra-cluster gas through gas ejection from Type II supernovae might proceed more efficiently in more massive GCs and consequently cause [Fe/H] spreads among GC stars. The present study suggests that simple GC-GC merging can also equally explain the observed [Fe/H] spreads in anomalous GCs.

(3) If the formation epochs of two GCs in dwarfs are separated by $\sim$ 300 Myr, then the chemical abundances of [Fe/H] and [Ba/Fe] can be different by 0.15 dex and 0.3 dex, respectively, owing to chemical enrichment by AGB stars and supernovae within the dwarfs. However, star formation in the GC-host dwarfs needs to proceed rather rapidly to obtain such rapid chemical enrichment, and the upper-mass cutoff ($m_{\rm upp}$) of IMF can influence the chemical evolution. The internal abundance spreads of merged GCs depend both on the star formation histories of their host dwarfs and on the time lag between two GC formation events. We suggest that star formation histories of dwarfs hosting anomalous GCs can be different from dwarfs hosting normal GCs. The observed no/little dependence of [Eu/Fe] on [Fe/H] in M22 is consistent with a scenario in which M22 was formed in a massive dwarf galaxy at a high redshift.

(4) Field stars can be captured by merged GCs in the central regions of GC-host dwarfs, if the mass-ratios of GCs to their hosts are large ($M_{\rm gc}/M_{\rm h}\sim0.0001$). The chemical abundances of these field stars should be different from those of stars initially in merging GCs. We suggest that metal-rich 'anomalous stars' observed in some GCs (e.g., NGC 6273; Johnson et al. 2015) can be formed as a result of tidal capture of field stars by merging GCs within dwarfs. As already discussed in BY12, stellar halos can be formed around merged GCs after tidal destruction of their host dwarfs.

(5) GC merger remnants inevitably show global rotation, because orbital angular momentum of merging GCs is converted into internal rotation of the remnants. The present study has investigated only merging of GCs with initially no net global rotation (i.e., dense stellar systems dynamically supported only by velocity dispersion) and found that the rotation amplitude is only $\sim1.5-6$ km s^{-1} for $M_{\rm gc}=10^6$ M$_\odot$. The stellar kinematics of GC merger remnants could depend on the initial stellar kinematics of merger progenitor GCs, which should be investigated in our future works.

(6) The details of chemical abundances in anomalous GCs can depend on the time lag between two GC formation events, the timescale of GC host destruction, and the chemical evolution processes of GC host dwarfs, if they were formed mainly from GC merging. The time lag between the formation epochs of two GCs that finally merge to form a single GC is very short for the case of NGC 1851 with little/no [Fe/H] spread whereas it should be at least a few Myr in the merger scenario of anomalous GCs with significant [Fe/H] spreads: GC merging alone does not necessarily form single anomalous GCs in this scenario.

ω Cen could possibly have experienced both multiple GC merging and gas inflow from the outer part of its host dwarf for a longer time scale so that it could have a very large [Fe/H] spread. The unique history of ω Cen needs to be discussed in detail by a separate paper.

We are grateful to the referee for his/her constructive and useful comments. T. T. is assisted in part by JSPS KAKENHI Grant Number 15K05033.

REFERENCES

Anderson, J., & King, I. R. 2003, AJ, 126, 772
Andrievsky, S. M., Luck, R. E., Martin, P., & Lépine, J. R. D. 2004, A&A, 413, 159
Bastian, N., Lamers, H. J. G. L. M., de Mink, S. E., Longmore, S. N., Goodwin, S. P., & Gieles, M. 2013, MNRAS, 436, 2398
Baumgardt, H., Kroupa, P., & Parmentier, G. 2008, 384, 1231
Bedin, L. R., Piotto, G., Anderson, J., Cassisi, S., King, I. R., Momany, Y., & Carraro, G. 2004, ApJ, 605, L125
Bekki, K. 2006, MNRAS, L367, 24
Bekki, K. 2007, PASA, 24, 77
Bekki, K. 2009, MNRAS, 399, 2221
Bekki, K. 2010a, ApJ, 724, L99
Bekki, K. 2010b, MNRAS, 401, 2753
Bekki, K. 2011, MNRAS 412, 2241 (B11)
Bekki, K. 2013, MNRAS, 432, 2298
Bekki, K. 2016, submitted to ApJ
Bekki, K., & Freeman, K. C. 2003, MNRAS, 346, L11
Bekki, K., Couch, W. J., Drinkwater, M. J., & Shioya, Y. 2003, MNRAS, 344, 399
Bekki, K., & Norris, J. E. 2006, ApJL 637, 109
Bekki, K. Campbell, S. W. Lattanzio, J. C., & Norris, J. E. 2007, MNRAS, 377, 335
Bekki, K., & Yong, D. 2012, MNRAS, 419, 2063 (BY12)
Bellazzini, M., et al. 2008, AJ, 136, 1147
Bellini, A., Piotto, G., Bedin, L. R., King, I. R., Anderson, J., Milone, A. P., & Momany, Y. 2009, A&A, 507, 1393
Carretta, E., 2015, ApJ, 810, 148
Carretta, E., et al. 2009, A&A, 505, 117
Carretta, E., et al. 2010, ApJ, 722, L1
Da Costa, G. S. Held, E. V. Saviane, I., & Gullieuszik, M. 2009, ApJ, 705, 1481
de Boer, T. J. L., et al. 2012, A&A, 544, 73
Conroy, C. & Spergel, D. N. 2011, ApJ, 726, 36
D'Antona, F., & Caloi, V. 2004, ApJ, 611, 871
D'Antona, F., & Caloi, V. 2008, MNRAS, 390, 693
D'Antona, F., Caloi, V., D'Ercole, A., Tailo, M., Vesperini, E., Ventura, P., & Di Criscienzo, M. 2013, MNRAS,
D'Antona, F., Vesperini, E., D'Ercole, A., Ventura, P., Milone, A. P., Marino, A. F., & Tailo, M. 2016, MNRAS, 458, 2122
de Boer, T. J. L., Belokurov, V., Beers, T. C., & Lee, Y . S. 2014a, MNRAS, 443, 658
de Boer, T. J. L., Belokurov, V., & Koposov, S. 2014b, MNRAS, 451, 3489
Decressin, T., Meynet, G., Charbonnel, C., Prantzos, N. & Ekström, S. 2007, A&A, 464, 1029
Da Costa, G. S., Held, E. V., Saviane, I., & Gullieuszik, M. 2009, ApJ, 705, 1481
D'Ercole, A., Vesperini, E., D'Antona, F., McMillan, S. L. W., & Recchi, S. 2008, MNRAS, 391, 825 (D08)
D'Ercole, A., D'Antona, F., Ventura, P., Vesperini, E., & McMillan, S. L. W. 2010, MNRAS, 407, 854
D'Ercole, A., D'Antona, F., & Vesperini, E. 2011, MNRAS, 415, 1304
Fenner, Y., Campbell, S., Karakas, A. I., Lattanzio, J. C., & Gibson, B. K. 2004, MNRAS, 353, 789
Gavagnin et al. 2016, MNRAS in press (arXiv:1606.02743)
Gratton, R. G., Carretta, E., & Bragaglia, A. 2012, A&ARv, 20, 50 (GCB12)
Hernquist, L., 1990, ApJ, 356, 359
Hidalgo-Gamez A. M., Ramirez-Fuentes D., Gonzalez J. J. , 2010, preprint (arXiv:1011.1013)
Johnson, C. I., Rich, R. M., Pilachowski, C. A., Caldwell, N., Mateo, M., Bailey, J. I. III., & Crane, J. D. 2015, AJ, 150, 63.
Lee, J-W., Kang, Y-W., Lee, J., & Lee, Y-W. 2009, Nature, 462, 480
Lee, J-W. 2015, ApJS, 219, 7
Lee, Y.-W., et al. 2005, ApJ, 621, L57
Lee, Y.-W., Joo, J.-M., Sohn, Y.-J., Rey, S.-C., Lee, H.-C., & Walker, A. R. 1999, Nature, 402, 55
Maoz, D., Mannucci, F., Li, W., et al. 2011, MNRAS, 421, 1508
Maxwell, A. J., Wadsley, J., Couchman, H. M. P., & Mashchenko, S. 2012, ApJ, 755, L35
McWilliam, A., Wallerstein, G., & Mottini, M. 2013, ApJ, 778, 149
Milone, A. P., Bedin, L. R., Piotto, G., & Anderson, J. 2009, A&A, 497, 755
Milone, A. P., Marino, A. F., Piotto, G., Bedin, L. R., Anderson, J., Renzini, A., King, I. R., Bellini, A., Brown, T. M., Cassisi, S., et al. 2015, MNRAS, 447, 927
Miyamoto, M., Nagai, R., 1975, PASJ, 27, 533
Marino, A. F. et al. 2011, A&A, 532, 8
Marino, A. F. et al. 2012, A&A, 746, 14
Marino, A. F. et al. 2015, MNRAS, 450, 815 (M15)
Marino, A. F., Milone, A. P., Casagrande, L., Collet, R., Dotter, A., Johnson, C. I., Lind, K., Bedin, L. R., Jerjen, H., Aparicio, A., & Sbordone, L. 2016, MNRAS, 459, 610
Marks, M., & Kroupa, P. 2010, MNRAS, 406, 2000
Milone, A. P., Bedin, L. R., Piotto, G., Marino, A. F., Cassisi, S., Bellini, A., Jerjen, H., Pietrinferni, A., Aparicio, A., & Rich, R. M. 2015, MNRAS, 450, 3750
Navarro, J. F., Frenk, C. S., White, & S. D. M. 1996, ApJ, 462, 563
Neto, A. F., Gao, Liang, Bett, P., Cole, S., Navarro, J. F., Frenk, C. S., White, S. D. M., Springel, V., & Jenkins, Adrian 2007, MNRAS, 381, 1450
Norris, J. E., & Da Costa, G. S. 1995, ApJ, 441, L81
Olszewski, E. W., Saha, A., Knezek, P., Subramaniam, A., de Boer, T., & Seitzer, P. 2009, AJ, 138, 1570
Piotto, G. et al. 2005, ApJ, 621, 777
Piotto, G. et al. 2007, ApJ, 661, L53
Salucci, P., & Burkert, A. 2000, ApJL, 537, 9
Shingles, L. J., Karakas, A. I., Hirschi, R., Fishlock, C. K., Yong, D., Da Costa, G. S., & Marino, A. F. 2014, ApJ, 795, 34
Tolstoy et al. 2004, ApJL, 617, 119
Tsujimoto, T. 2011, ApJ, 736, 113 (T11)
Tsujimoto, T., & Bekki, K. 2011, A&A, 530, 78
Tsujimoto, T., & Bekki, K. 2013, MNRAS, 436, 1191
Tsujimoto, T. & Shigeyama, T. 2014, ApJ, 795, L18
Vesperini, E. 1997, MNRAS, 287, 915
Vesperini, E., McMillan, S. L. W., D'Antona, F., & D'Ercole, A. 2010, ApJ, 718, L112
Yong, D., Grundahl, F., D'Antona, F., Karakas, A. I., Lattanzio, J. C., & Norris, J. E. 2009, ApJ, 695, L62
Yong, D., et al. 2013, MNRAS, 434, 3542
Yong, D., Roederer, I. U., Grundahl, F., Da Costa, G. S., Karakas, A. I., Norris, J. E., Aoki, W., Fishlock, C. K., Marino, A. F., Milone, A. P., & Shingles, L. J. 2014, MNRAS, 441, 3396
Yong, D., Grundahl, F., & Norris, J. E. 2015, MNRAS, 446, 3319

TABLE 1
DESCRIPTION OF THE PARAMETER VALUES FOR THE REPRESENTATIVE FOUR MODELS.

ID [a]	$m_{\rm FG,1}$ [b]	$a_{\rm FG,1}$ [c]	m_2 [d]	$R_{\rm gc,1}$ [e]	$R_{\rm gc,2}$ [f]	Dwarf [g]	Orbit [h]	$t_{\rm merge}$ [i]	Comment [j]
M1	1.0	10.0	1.0	100	200	D1	O1	0.31	Fiducial
M2	1.0	10.0	1.0	200	400	D1	O1	0.30	
M3	1.0	10.0	1.0	400	600	D1	O1	1.33	
M4	1.0	10.0	1.0	600	800	D1	O1	N	
M5	0.3	5.8	1.0	100	200	D1	O1	N	
M6	0.1	3.2	1.0	100	200	D1	O1	N	
M7	1.0	10.0	0.1	100	200	D1	O1	N	Unequal-mass
M8	1.0	1.0	1.0	100	200	D2	O1	0.52	FG-only
M9	0.3	5.8	1.0	100	200	D2	O1	1.34	
M10	1.0	10.0	1.0	100	200	D2	O1	0.18	
M11	1.0	10.0	1.0	100	200	D3	O1	N	
M12	1.0	10.0	1.0	100	200	D1	O1	0.41	FG-only
M13	–	–	–	–	–	D4	O1	–	No GCs
M14	1.0	10.0	1.0	100	200	D1	O3	1.73	Young MW
M15	0.3	5.8	1.0	100	200	D1	O3	0.74	
M16	1.0	10.0	1.0	100	200	D1	O4	0.54	
M17	1.0	10.0	1.0	100	200	D5	O1	0.32	SB profile
M18	1.0	10.0	1.0	100	200	D1	O2	1.25	Distant orbit
M19	1.0	10.0	1.0	100	200	D6	O1	–	No GC

[a] The host dwarf galaxy model (e.g., D1) and orbital model (e.g. O1) are given in Table 2 and 3, respectively. The fiducial model adopts D1, and O1, and NFW dark matter model. The mass-ratio of SG to FG stellar systems are 0.2 for all models with FG+SG systems. GCs with only FG systems are clearly indicated as 'FG-only' in the comment column.

[b] The initial total mass of FG stars of GC1 in units of $10^6 M_\odot$.

[c] The scale-length of a FG systems ($a_{\rm FG,1}$) in a GC1. The scale-length of the SG is $0.2a_{\rm FG,1}$.

[d] The mass-ratio of GC2 to GC1.

[e] The initial distance of GC1 from the Galactic center in units of pc.

[f] The initial distance of GC2 from the Galactic center in units of pc.

[g] The host dwarf galaxy model.

[h] The orbital evolution model around the Galaxy.

[i] 'N' means that two GC1 and GC2 can not merge with each other before the completion of tidal destruction of their host dwarf galaxy. The value given in each model is $t_{\rm merge}$ in units of Gyr (the timescale of GC merging). '−' means that GC merging can not be defined owing to no GCs in the model.

[j] Comments on each model, if any.

TABLE 2
DESCRIPTION OF THE PARAMETER VALUES FOR GC-HOST DWARF GALAXIES.

Model ID [a]	$M_{\rm h}$ [b]	$r_{\rm vir}$ (kpc) [c]	$M_{\rm s}$ [d]	$r_{\rm s}$ (kpc) [e]	DM profile [f]	GC [g]
D1	1.0	9.2	1.5	1.3	NFW	Yes
D2	0.3	5.0	0.45	0.7	NFW	Yes
D3	3.0	15.9	4.5	2.3	NFW	Yes
D4	1.0	9.2	1.5	1.3	NFW	No
D5	1.0	9.2	1.5	1.3	SB	Yes
D6	0.01	0.92	0.015	0.13	NFW	No

[a] These model IDs are used in Table 1.

[b] The initial total mass of the dark matter halo ($M_{\rm h}$) of a GC-host dwarf in units of $10^{10}M_{\odot}$.

[c] The virial radius of the dark matter halo of a GC-host dwarf. in units of kpc.

[d] The initial total mass of the stellar disk of a GC-host dwarf in units of $10^{8}M_{\odot}$.

[e] The initial size of the stellar disk of a GC-host dwarf in units of kpc.

[f] NFW and SB represents the NFW and SB profiles, respectively, for the initial radial density distributions of dark matter halos.

[g] 'Yes' ('No') means that a dwarf galaxy (does not) have GCs.

TABLE 3
MODEL PARAMETERS FOR THE THREE-COMPONENT GALACTIC POTENTIALS AND DWARF ORBITS.

Model ID [a]	$M_{\rm disk}$ [b]	$M_{\rm bulge}$ [c]	$v_{\rm halo}$ [d]	$R_{\rm i}$ [e]	$f_{\rm v}$ [f]
O1	10.0	3.4	131.5	17.5	0.5
O2	10.0	3.4	131.5	35.0	0.5
O3	1.0	0.34	93.0	17.5	0.5
O4	1.0	0.34	93.0	8.8	0.7

[a] The first two models (O1 and O2) correspond to the present Galaxy whereas other two (O3 and O4) mimic the early formation phase of the Galaxy (before/during the formation of the first thin disk).

[b] The initial stellar disk mass of the Galaxy in units of $10^{10}M_{\odot}$.

[c] The initial stellar bulge mass of the Galaxy in units of $10^{10}M_{\odot}$.

[d] The velocity parameter in the adopted logarithmic potential of the Galactic halo in units of km s^{-1}.

[e] The initial distance of a dwarf from the Galactic center in units of kpc.

[f] The circular velocity factor: $f_{\rm v} = 1$ means that the velocity of a dwarf is the same as the circular velocity at its initial location.

APPENDIX

POSSIBLE INFLUENCES OF STELLAR GALACTIC NUCLEI ON THE TIMESCALE OF GC MERGING

Although stellar galactic nuclei (SGN) are included in the initial dwarf disk models by BY12, they are not modeled in the present study. The initial presence of SGN might be able to influence the GC merging processes in dwarfs significantly. We have therefore investigated how SGN can influence the orbits of two GCs in the fiducial model by assuming that the initial masses of SGN ($M_{\rm nuc}$) are either $10^5 M_\odot$ or $10^6 M_\odot$. The SGN is modeled by a point-mass particle with $M_{\rm nuc}$ rather than by a self-gravitating system in this investigation. Given that the initial stellar mass in the fiducial model ($M_{\rm s}$) is $1.5 \times 10^8 M_\odot$, the adopted $M_{\rm nuc}$ ($0.15 - 1.5\%$ of $M_{\rm s}$) is quite reasonable. Figure 12 shows that the GC merging timescale ($t_{\rm merge}$) is not so different between these two models with SGN and the fiducial one (M1). The two GCs in these models merge with each other within 0.7 Gyr ($t_{\rm merge} = 0.45$ Gyr for $M_{\rm nuc} = 10^6 M_\odot$ and $t_{\rm merge} = 0.64$ Gyr for $M_{\rm nuc} = 10^5 M_\odot$). The presence of SGN can slightly lengthen GC merging (by $0.1 - 0.3$ Gyr depending $M_{\rm nuc}$) owing to dynamical interaction between SGN and each of the two GCs. We therefore suggest that $t_{\rm merge}$ can not be significantly influenced by the presence of SGN in dwarf disk galaxies.

TABLE 4
FIVE KEY PARAMETERS THAT DETERMINE THE LEVELS OF CHEMICAL ABUNDANCE SPREADS IN GCS.

Key parameter [a]	Description [b]
$M_{\rm h,th}$	A threshold host halo mass for GC formation
$m_{\rm g,th}$	A threshold GC mass for GCs with multiple stellar populations
$t_{\rm merge}$	Timescale of GC merging
$t_{\rm dest}$	Timescale of dwarf destruction by the Galactic tidal field
$f_{\rm m,gc}$	The mass-ratio of one GC to its host halo

[a] These are *possible* five key parameters that are used to divide GCs into different types (i.e., different degrees of abundance inhomogeneity). There would be other important parameters for the origin of multiple stellar populations in GCs.

[b] The details of the physical meanings of these parameters are given and discussed in the main text.

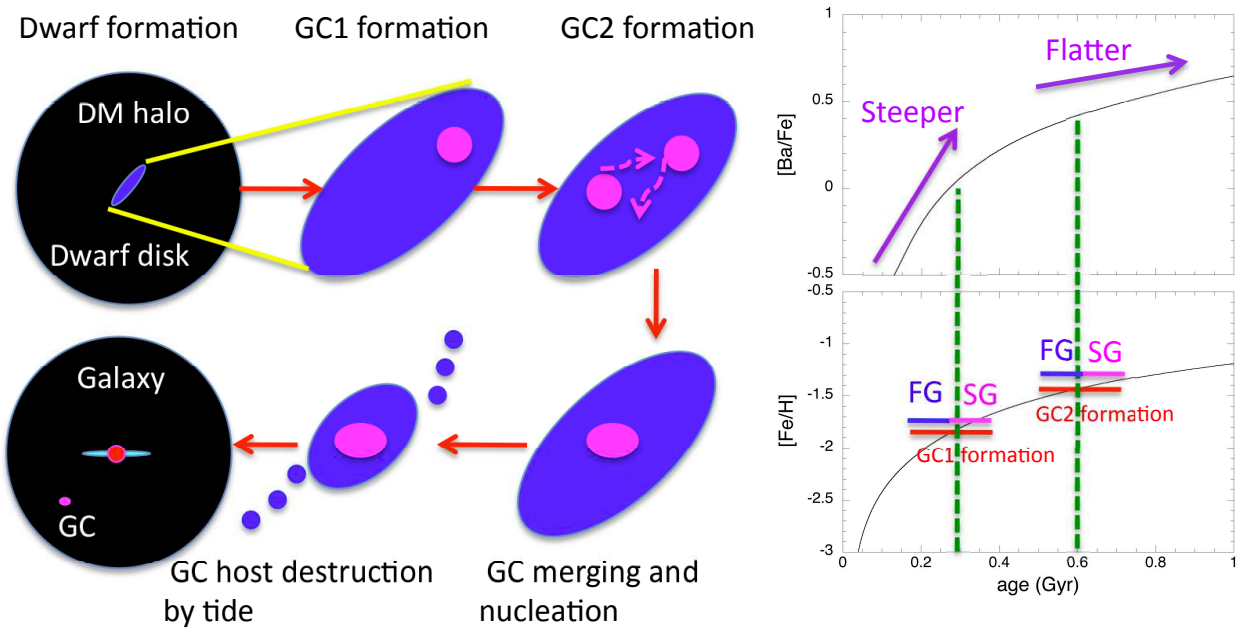

FIG. 1.— An illustrative figure for the 'GC merging' scenario for the origin of anomalous GCs with metallicity spreads. In this scenario, two GCs (GC1 and GC2) were formed from gas clouds within a dwarf galaxy embedded in a massive dark matter halo at different epochs. The two GCs lose orbital energy and angular momentum due to dynamical friction against field star of the dwarf so that they can spiral into the nuclear region of the dwarf. The two GCs consequently merge with each other to form an off-center nucleus (or new nuclear GC). The dwarf galaxy can be completely destroyed by the tidal field of the Galaxy during its accretion onto the Galactic halo. The new GC can survive from the tidal destruction, and thus is identified as a Galactic halo GC. Each of the two GCs have FG and SG stars, the two GCs have different [Ba/Fe] and [Fe/H] because they are formed at different epochs. If the formation epochs of the two GCs are separated by ~ 300 Myr, then [Fe/H] and [Ba/Fe] can be different by 0.2 dex and 0.3 dex, respectively, between the two GCs as a result of chemical evolution of the dwarf. Therefore, the new GC formed from merging of the two GCs should have abundance spreads both in [Fe/H] and [Ba/Fe]. The [Ba/Fe]-[Fe/H] relation becomes flatter at later times, which can be reflected on the abundance patterns of massive GCs such as ω Centauri.

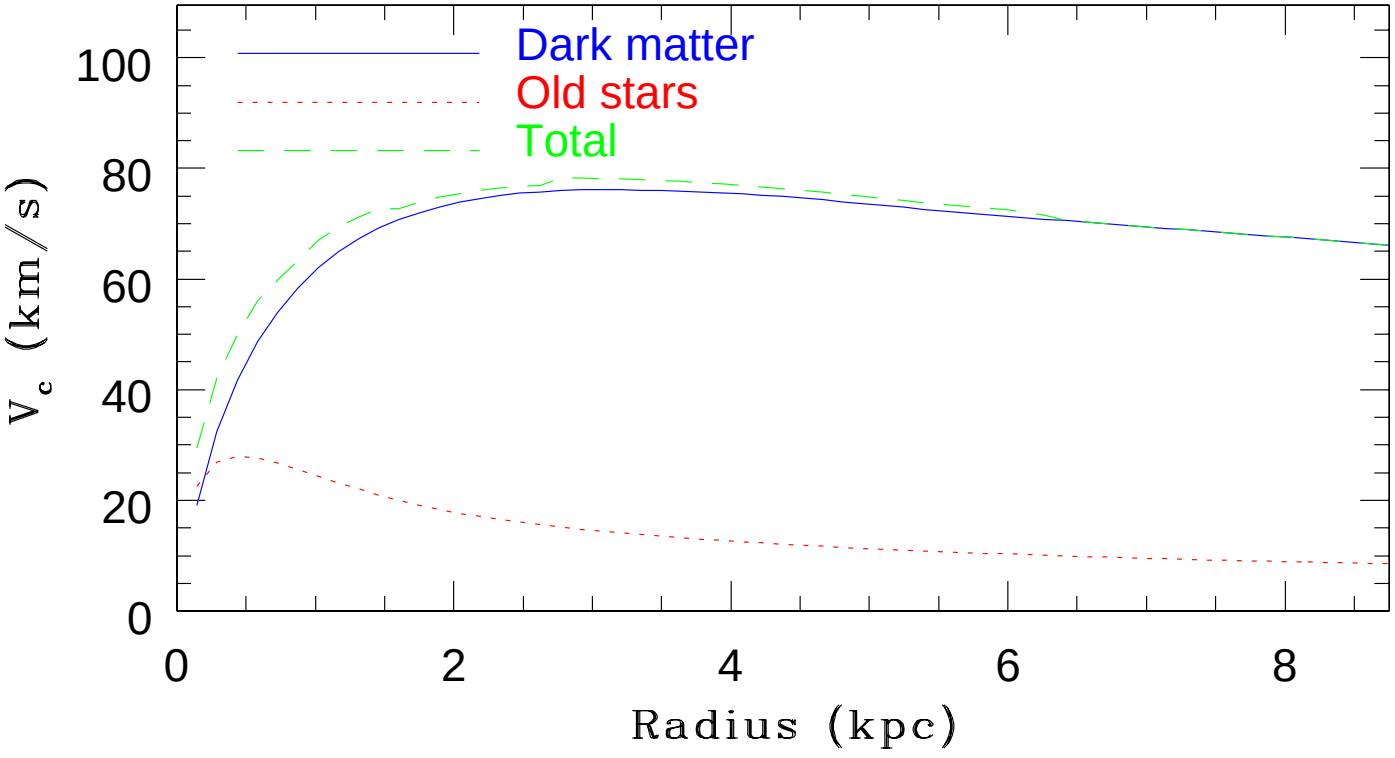

FIG. 2.— The contributions of dark matter (blue solid), old stars (red dotted), and all components (green dashed) to the circular velocity curve of the dwarf disk galaxy model D1.

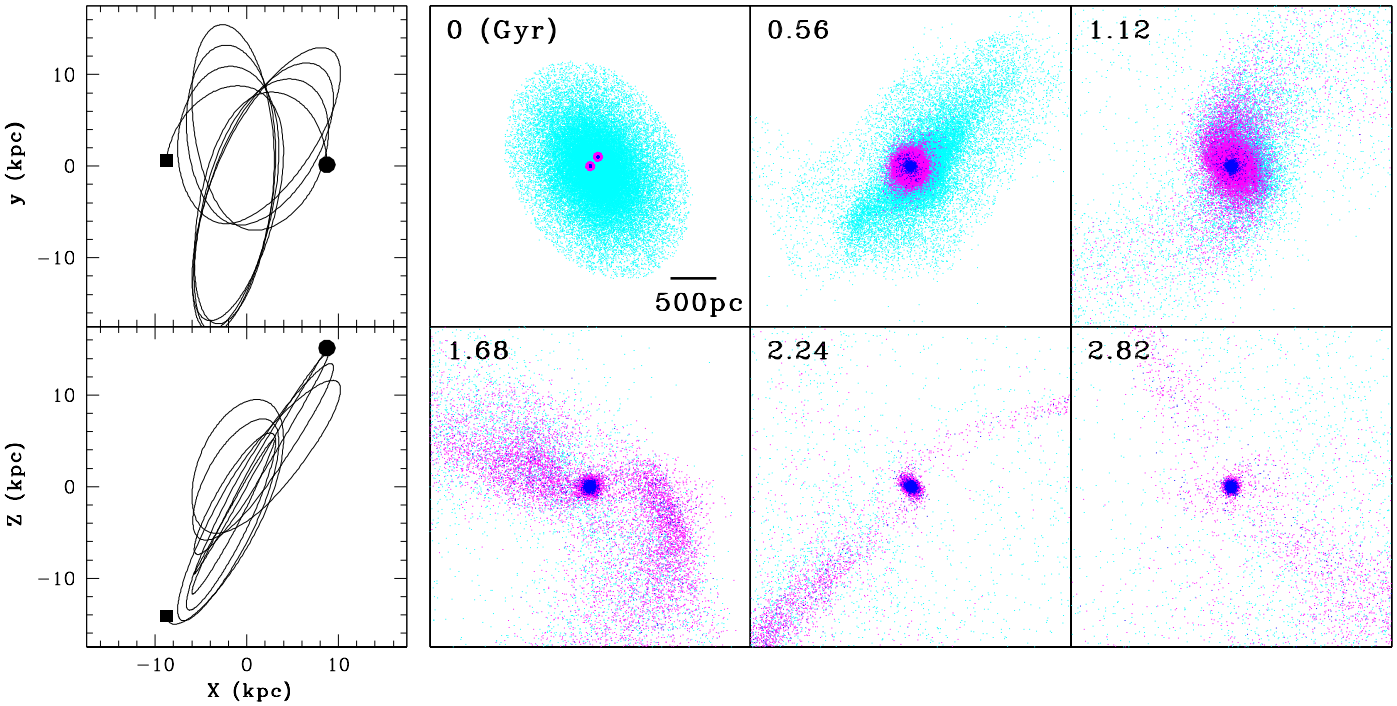

FIG. 3.— The left two panels show the orbit of a dwarf projected onto the x-y (upper) and x-z planes (lower) for the orbital model O1. The initial and final locations of the dwarf are indicated by filled circles and squares, respectively. The right six panels show the time evolution of the mass distributions of the dwarf and its two GCs projected onto the x-y in the fiducial model M1 with O1 orbital model. Disk (old) stars, FG stars, and SG stars are shown by cyan, magenta, and blue, respectively. The time T that has elapsed since simulation started is shown in the upper left corner of each panel. Only one in ten disk particles is shown so that the file size of this figure can be significantly reduced (yet the key results can be clearly seen).

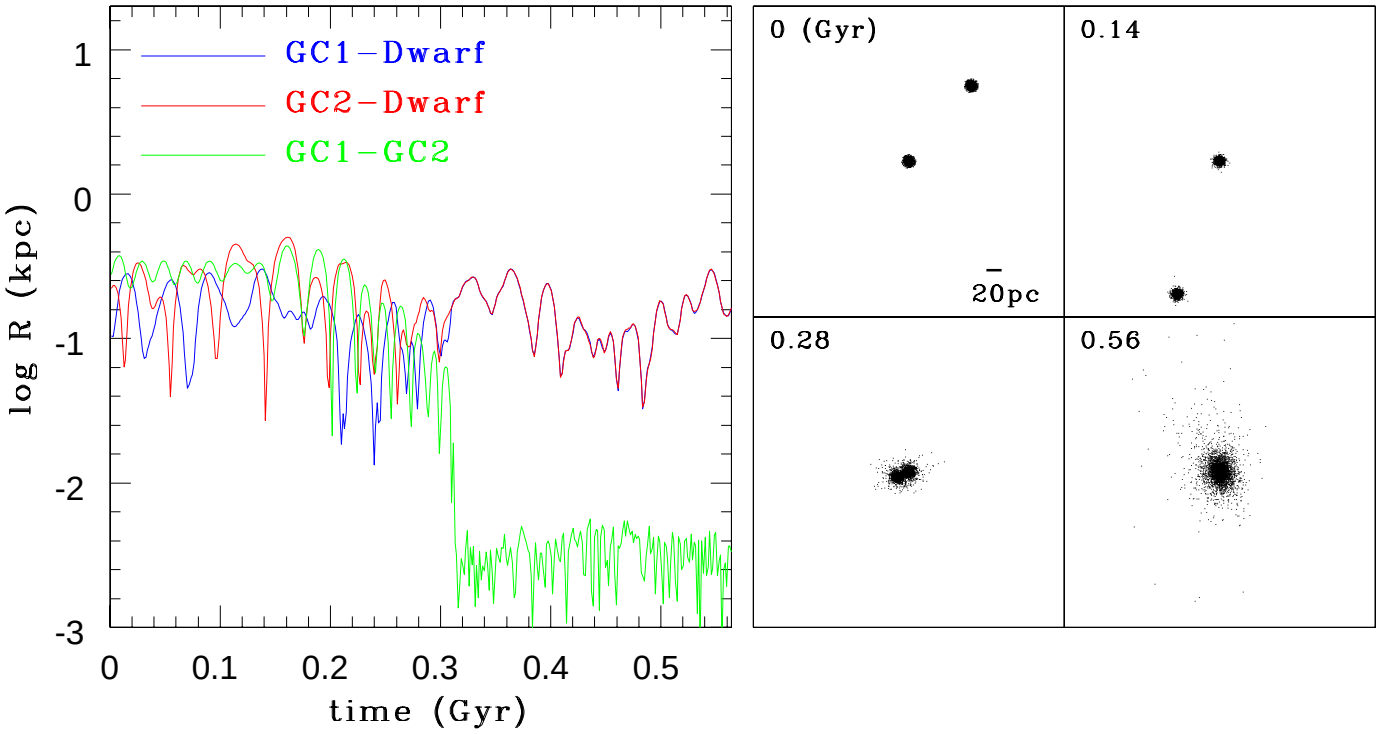

FIG. 4.— The bigger left panel shows the time evolution of the distance (R) between a GC-host dwarf and GC1 (blue), the host and GC2 (red), and GC1 and GC2 (green) in the fiducial model M1. The smaller four right panels describe the mass distribution of SG stars in GC1 and GC2 projected onto the x-y plane in the fiducial model at our selected time steps. The epoch of GC-merging corresponds to the point where the GC1-GC2 distance becomes rather small ($R < 3$ pc) suddenly and dramatically (i.e., $T \sim 0.3$ Gyr). The 'center' of the dwarf is defined as the position of the nuclear particle, and the GC-dwarf distance is measured using the position of each GC and that of the nuclear particle. Since the nuclear particle is moving in the central region of the dwarf, the GC1-dwarf distance can be still large even after the merged GCs can spiral in the nuclear region of the dwarf.

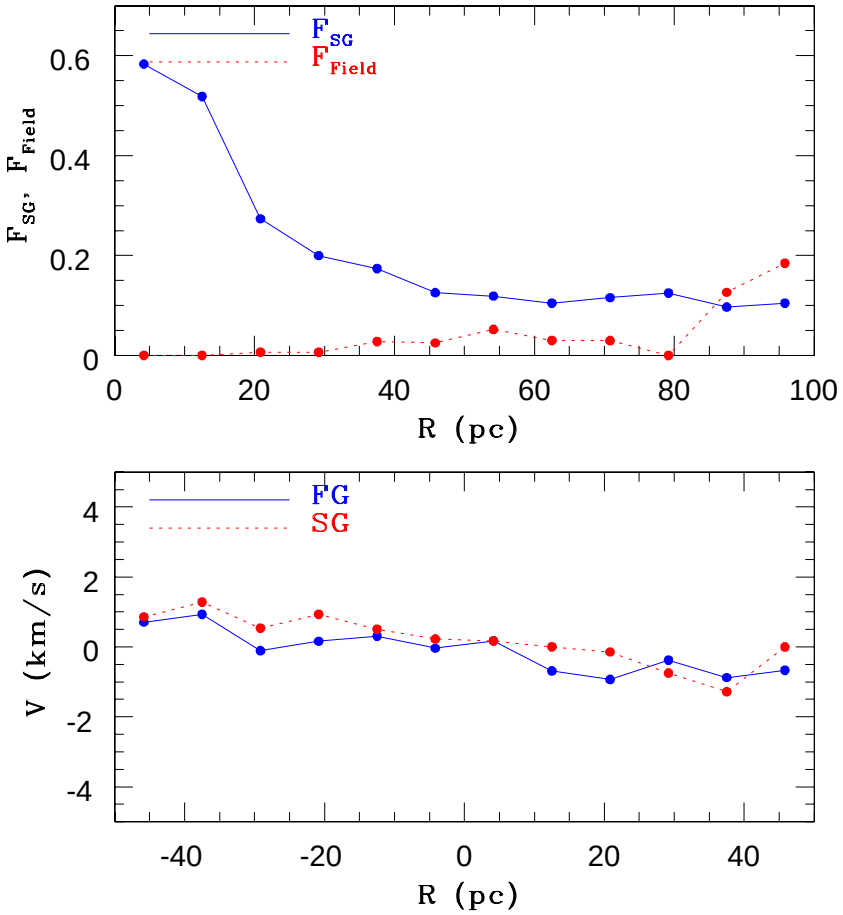

FIG. 5.— The upper panel shows the radial dependence of the mass-ratio of SG to FG stars ($F_{\rm SG}$; blue solid) and that of field to FG stars ($F_{\rm FG}$) in the new GC formed from major GC merging in the fiducial model M1 The lower panel shows the rotation curve profiles along the y-axis for FG (blue solid) and SG stars (red dashed) in the new GC.

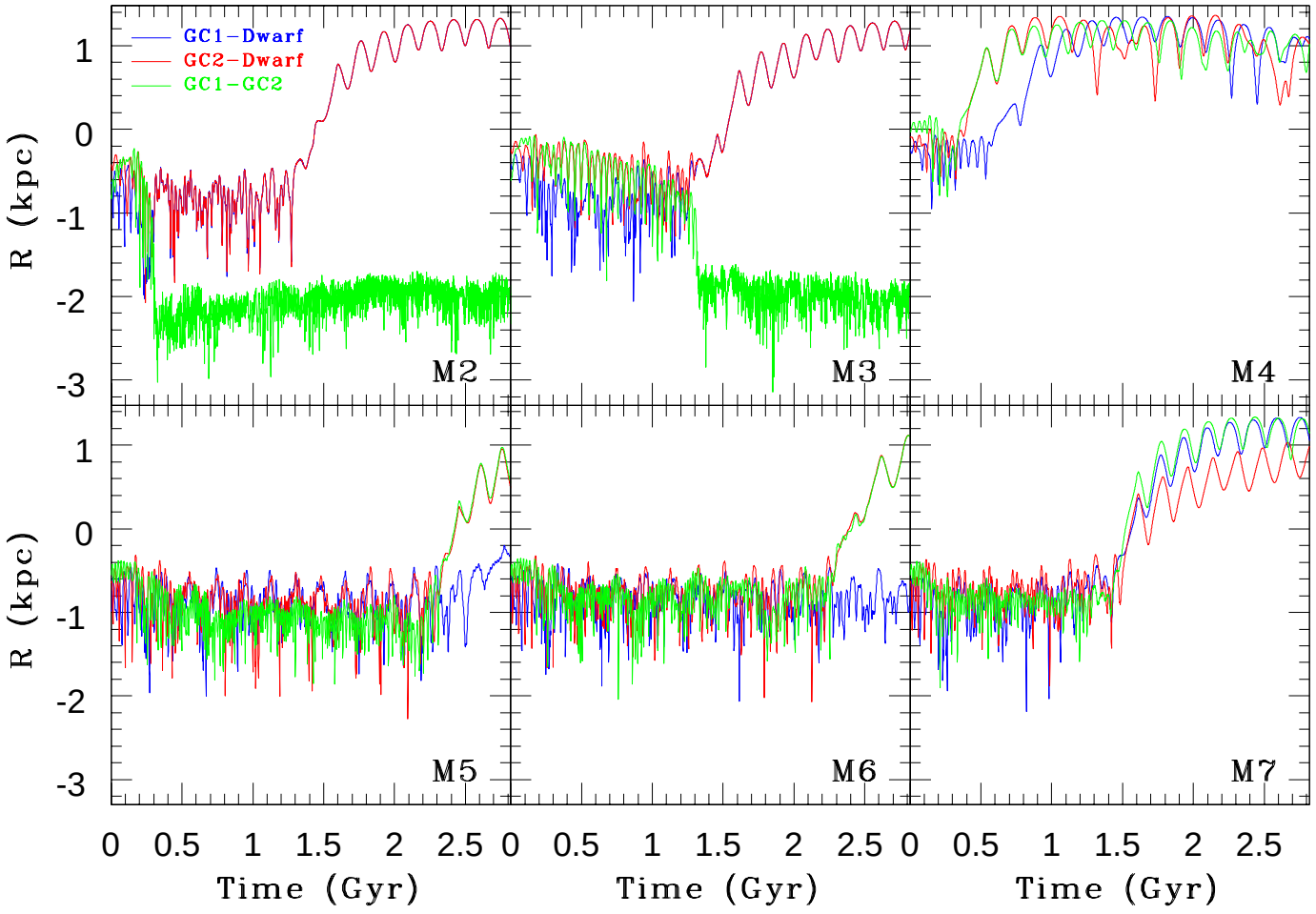

FIG. 6.— The same as the left panel of Figure 4 but for 6 different models (M2-M7). The epoch when the merged GC (or either/both of the two GCs) is stripped from the host dwarf galaxy corresponds to the point where the GC-dwarf distance (red or blue line) become suddenly large ($R > 1$ kpc). Clearly, GC merging is possible in M2, M3, and M5, whereas it is not in M6 and M7, in which at least one of the two GCs has a low mass ($m_{\rm FG,1} = 10^5 {\rm M}_\odot$).

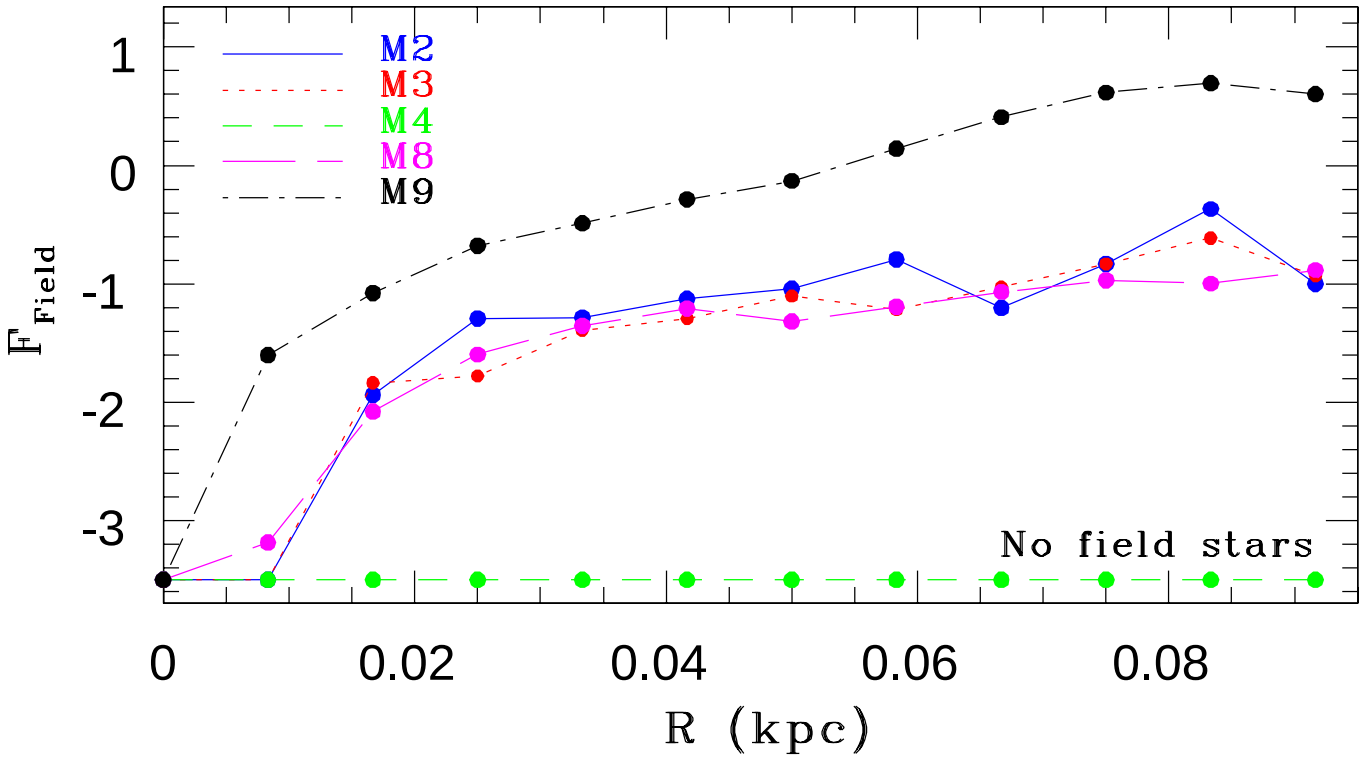

FIG. 7.— The mass-ratio of field to FG stars ($F_{\rm Field}$) for different models, M2 (blue solid), M3 (red dotted), M4 (green dashed), M8 (magenta long-dashed), and M9 (black dot-dashed). For convinience, $\log F_{\rm Field} = -3.5$ means no field stars around the GCs. Accordingly, the model M4 does not show any field stars in the halo of the GC.

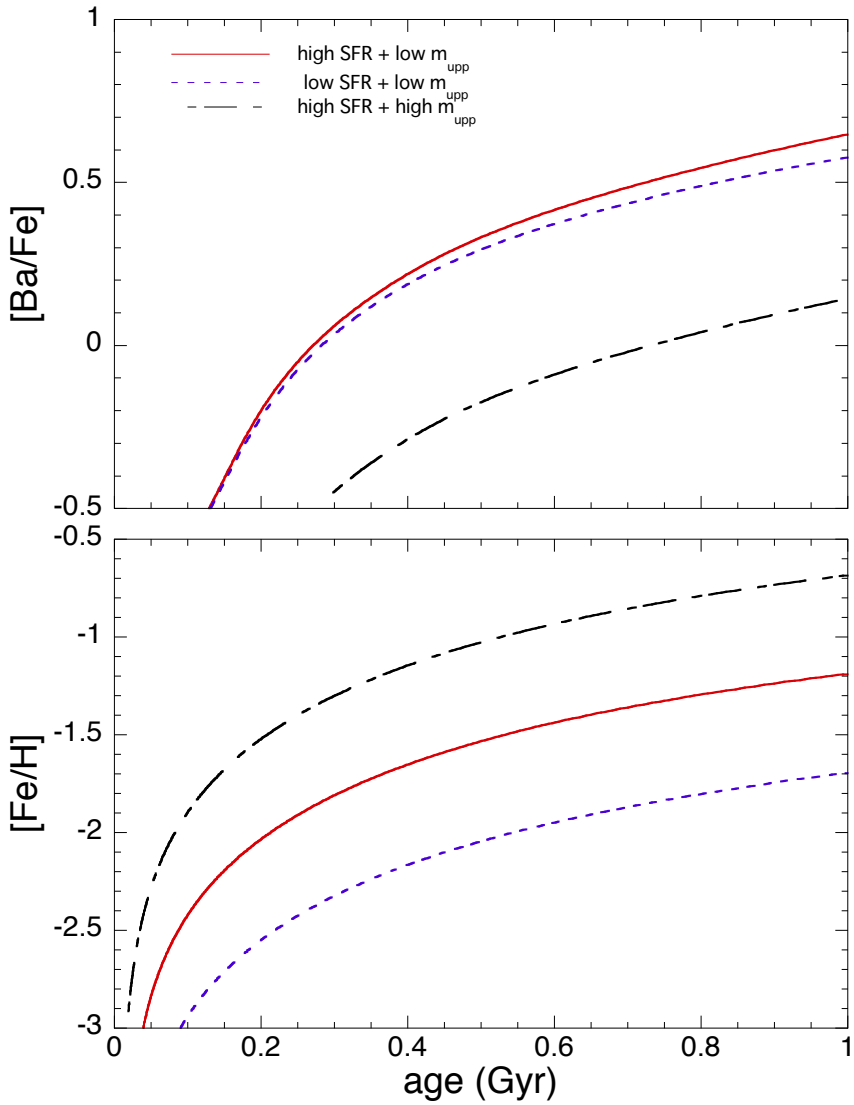

FIG. 8.— The time evolution of [Ba/Fe] (upper) and [Fe/H] (lower) in the three chemical evolution models with different star formation histories and upper cut-off stellar masses of the adopted IMF ($m_{\rm upp}$): high star formation rate with low $m_{\rm upp}$ (red solid), low star formation rate with low $m_{\rm upp}$ (blue short-dashed), and high star formation rate with low $m_{\rm upp}$ (black dot-dashed). The physical meanings of 'low' and 'high' star formation rate models are given in the main text.

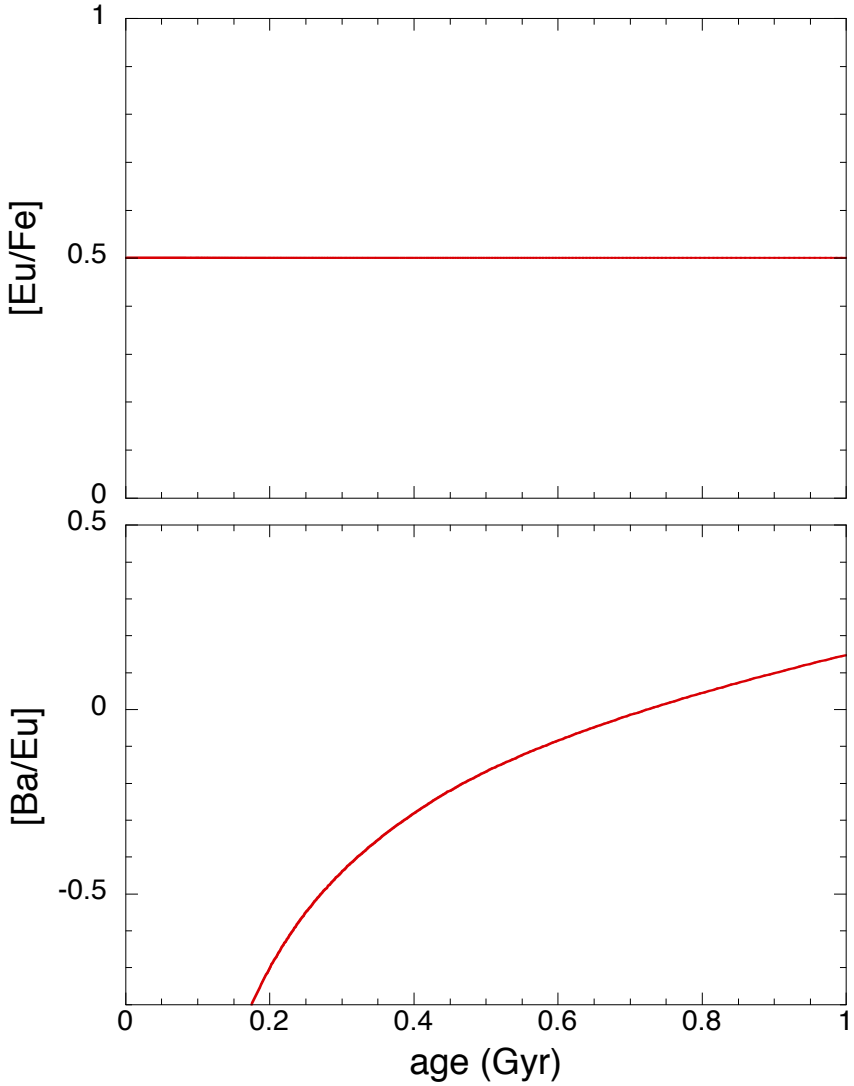

FIG. 9.— The same as Figure 8 but for [Eu/Fe] (upper) and [Ba/Eu] (lower) for the best model. The implication of the flat [Eu/Fe] evolution is given in the main text.

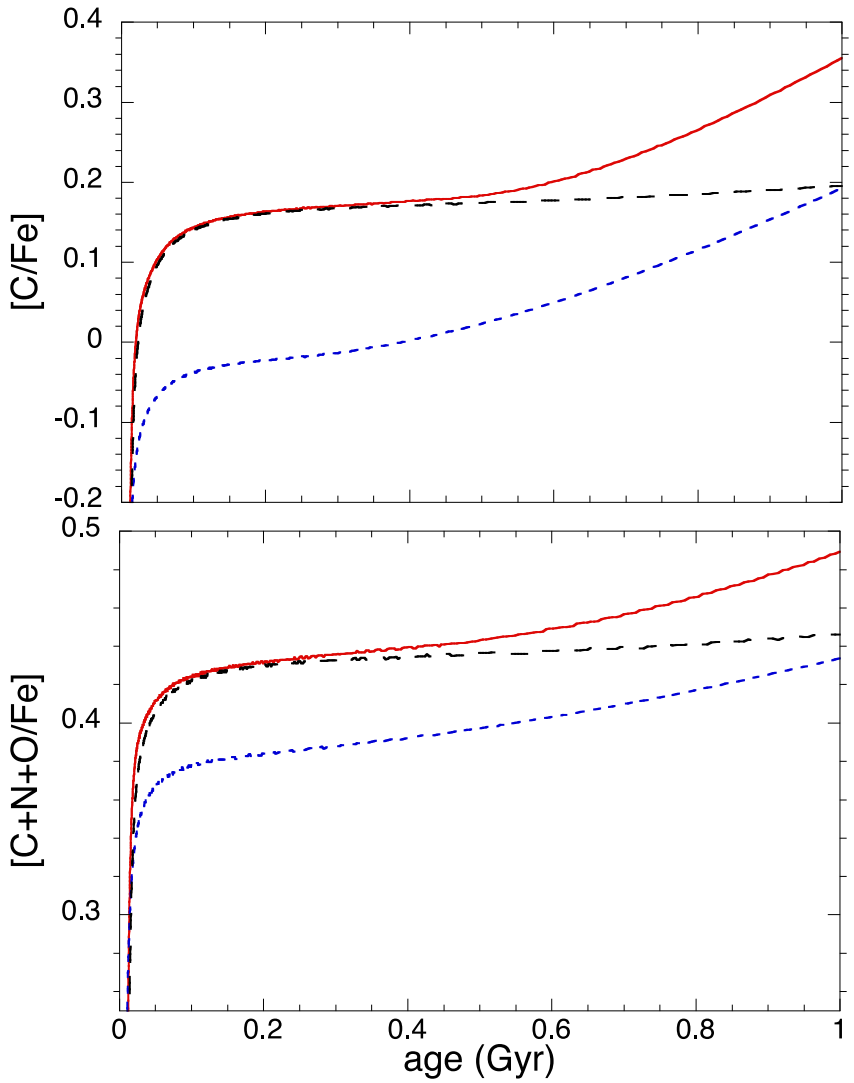

FIG. 10.— The same as Figure 8 but for the evolution of C (upper) C+N+O (lower) for the three models.

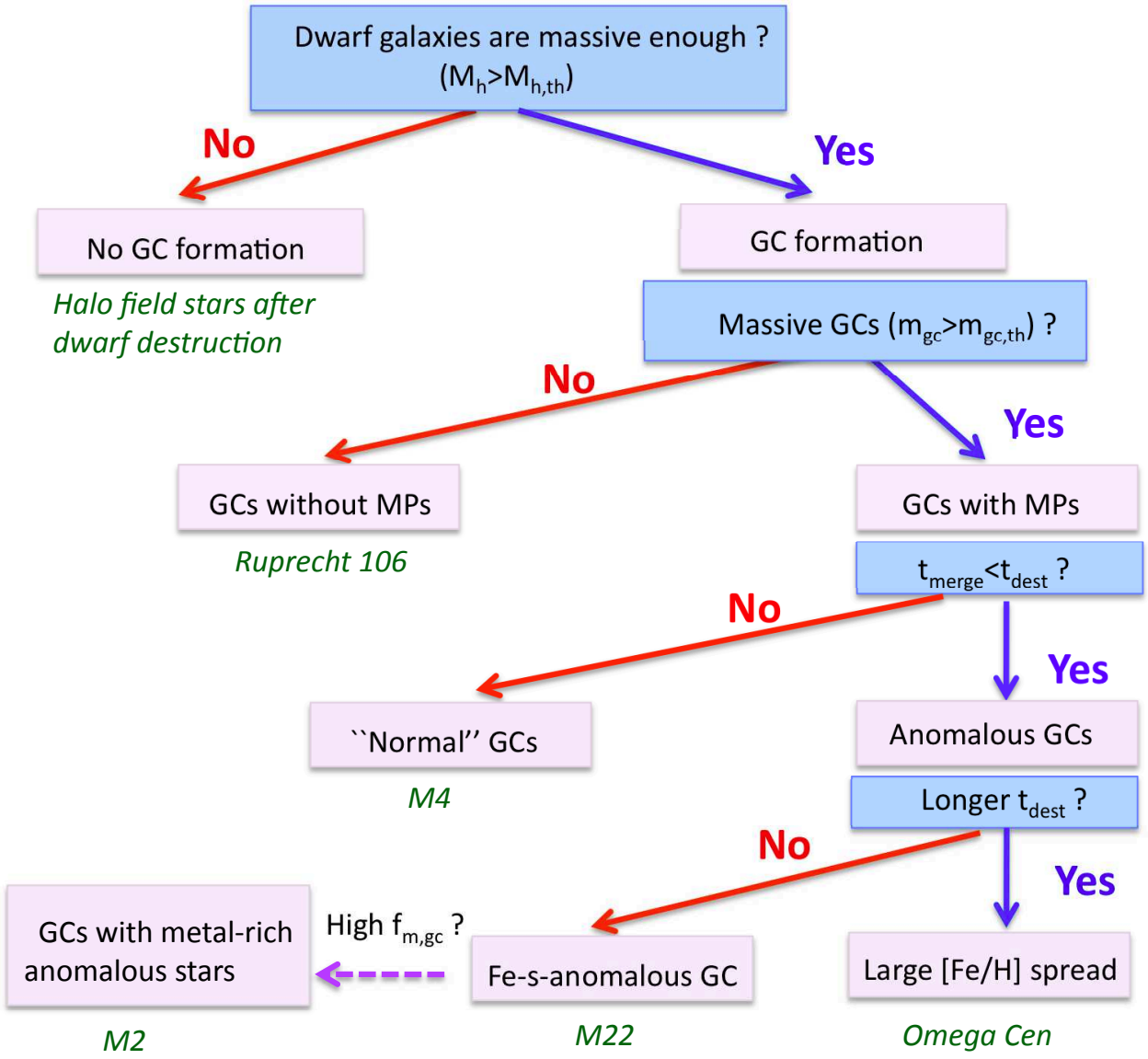

FIG. 11.— A schematic diagram for an unified picture of GC formation with multiple stellar populations (MPs). There are five key parameters in this diagram, $M_{\rm h,th}$ (threshold dwarf mass for GC formation), $m_{\rm gc,th}$) (threshold GC mass for GC formation with MPs), $t_{\rm merge}$ (timescale for GC merging), $t_{\rm dest}$ (timescale of dwarf destruction), and $f_{\rm m,gc}$ (mass ratio of a GC to its host halo). GCs can be divided into different categories (e.g., GCs without MPs and anomalous GCs) according to whether or not they meet the four specific criteria (e.g., '$t_{\rm merge} < t_{\rm dest}$'). It should be stressed here that merging of two GCs does not necessarily lead to the formation of a single anomalous GCs, because the two GCs need to form at different epochs within their host dwarf. Both M22 and NGC 1851 can be formed from GC merging, but the difference in the formation epochs between two GCs for NGC 1851 is small. Accordingly, NGC 1851 can not become an anomalous GC with a significant [Fe/H] spread. The extensive discussion on GC formation based on this diagram is given in the main text.

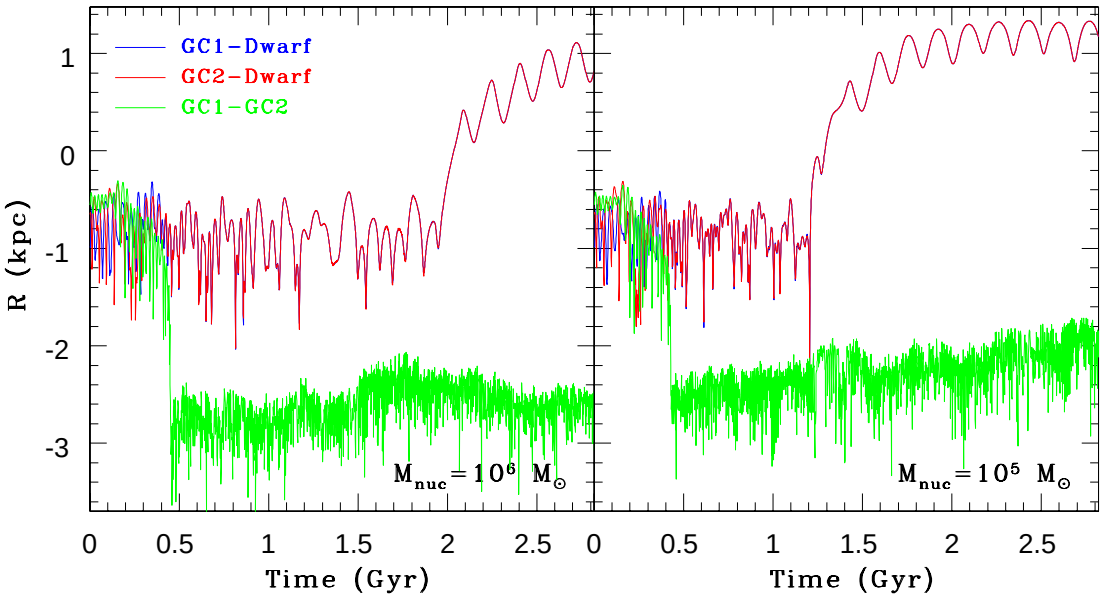

FIG. A12.— The same as Figure 6 but for the two models with $M_{\rm nuc} = 10^6 M_\odot$ (left) and $M_{\rm nuc} = 10^5 M_\odot$ (right), $M_{\rm nuc}$ is the mass of the stellar galactic nucleus in the dwarf galaxy for the standard dwarf model (D1).